

Astrophysical Objects

Active Galaxies

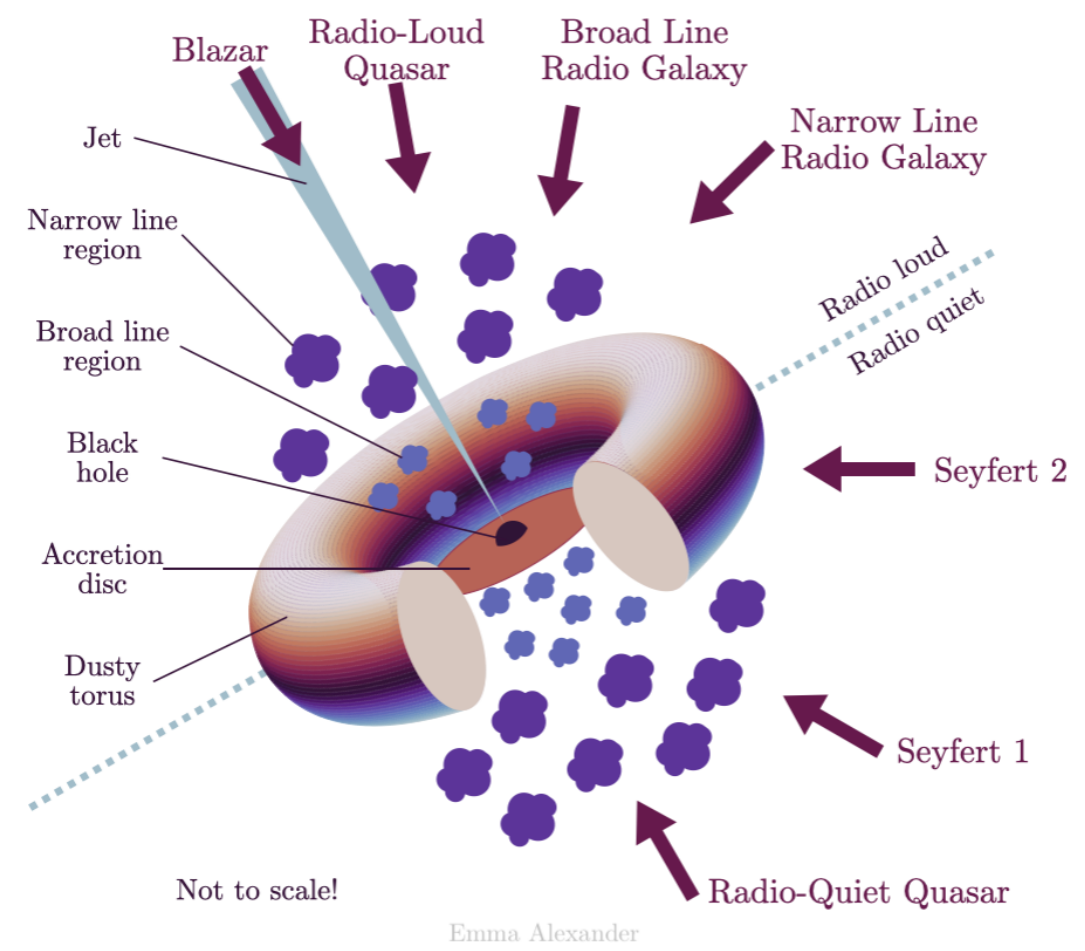
Based on: An introduction to modern Astrophysics chapter 28

Helga Dénés 2023 S2 Yachay Tech
hdenes@yachaytech.edu.ec



**SCHOOL OF
PHYSICAL SCIENCES
AND NANOTECHNOLOGY**

Unified model of AGN



There were **many similarities in the different types of AGN**, such as a bright compact nucleus, a wide continuum, and time variability, there were **also many differences**, including the presence or absence of broad emission lines, and the strength of radio and X-ray emission. The question is: **Are the types of AGNs fundamentally different or fundamentally the same?**

It now seems likely that active galactic nuclei are all powered by the **same general engine, accretion onto central supermassive black holes**. Accordingly, the observational differences are due to the different orientations of the objects as viewed from Earth and to the different rates of accretion and masses of the central black holes. The presence of radio lobes is then something in addition to, and consistent with, the basic model.

The model does serve to provide a framework for organizing the observations of AGNs and their interpretations. Successful predictions have been made on the basis of the idea of unification, and it appears that the basic features of a unified model of AGNs are in hand.

Unified model of AGN

Two pieces of evidence suggesting that the unified model is justified.

Figure 21 shows $L_{\text{H}\alpha}$, the luminosity in the $\text{H}\alpha$ emission line, and L_{FC} , the luminosity of the featureless continuum at a wavelength near 480 nm, plotted for a variety of AGNs (excluding blazars).

If the hydrogen emission lines are produced via the **photoionization of hydrogen atoms by the continuum radiation and the atoms' subsequent recombination**, then **the two luminosities should be proportional**, and a straight line with a slope of 1 should be found on a log–log graph. The slope of the dashed line is 1.05, confirming that $L_{\text{H}\alpha} \propto L_{\text{FC}}$. This result **implies a common origin for the hydrogen emission lines**, both broad and narrow, that are observed in AGNs for Seyfert 1 and 2 galaxies, broad- and narrow-line radio galaxies, and radio-loud and radio-quiet quasars.

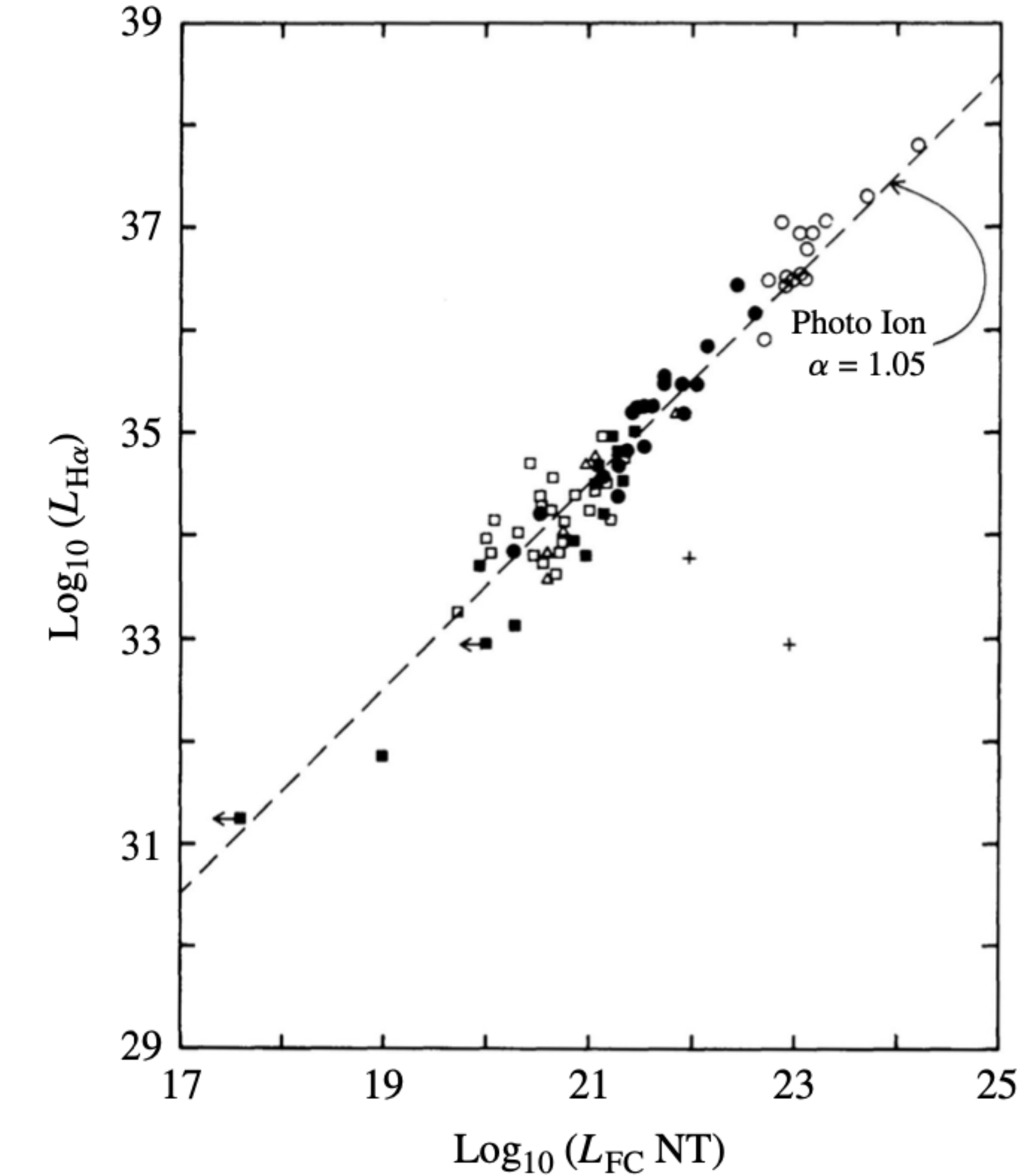


FIGURE 21 The luminosity in the $\text{H}\alpha$ emission line versus the luminosity of the featureless continuum at a wavelength near 480 nm (the “NT” stands for “nonthermal”). The symbols are quasars (open circles), Seyfert 1s (filled circles), Seyfert 2s (open squares), NLRGs (triangles), and more Seyfert 2s and NLRGs (filled squares). (Figure adapted from Shuder, *Ap. J.*, 244, 12, 1981.)

Unified model of AGN

Another piece of evidence : Observations of **NGC 1068 (a Seyfert 2) in polarized light**, they **found a Seyfert 1 spectrum with broad emission lines**.

This and similar cases discovered since then imply that **within these Seyfert 2s are Seyfert 1 nuclei that are hidden from the direct view of Earth by some optically thick material**. The diminished Seyfert 1 spectrum (normally overwhelmed by the direct Seyfert 2 spectrum) **comes from light that reaches us indirectly by reflection from the interstellar medium outside the nucleus**. This reflection would also **contribute to the observed linear polarization**, when the electric field vector is perpendicular to the radio axis.

The **orientation of the AGN relative to the line of sight** from Earth is an important factor in the unified model.

Unified model of AGN

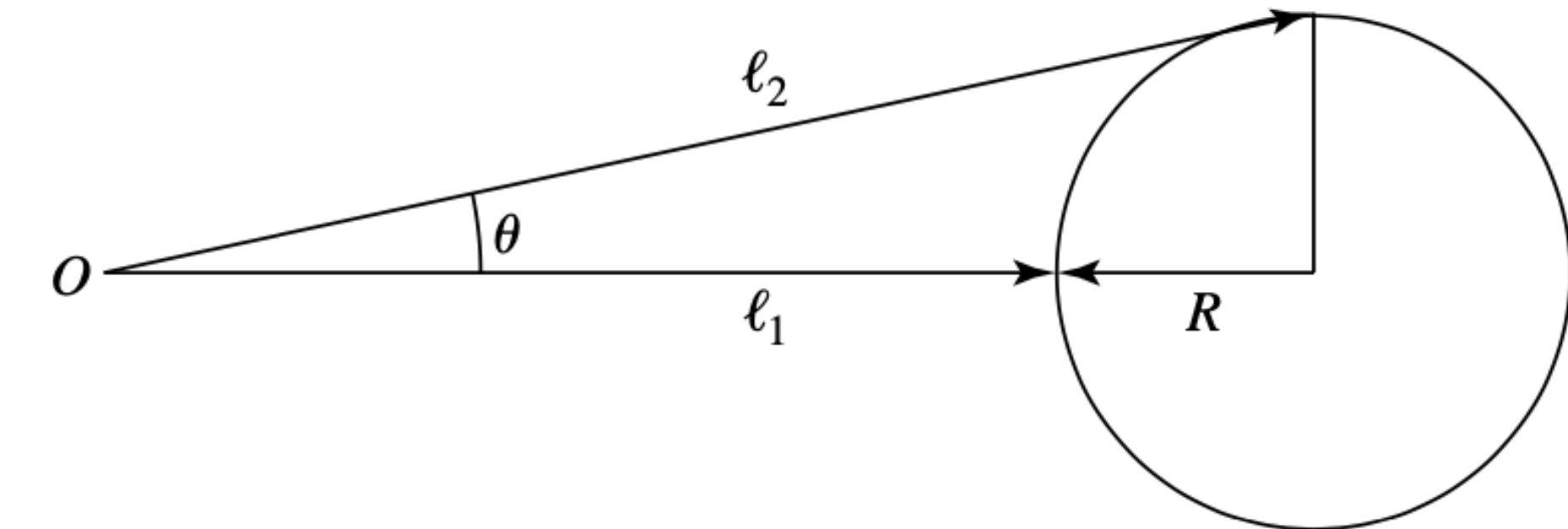


FIGURE 22 The brightening of a sphere as seen by a distant observer at point O .

The **most important clue** to the nature of the central engine that powers AGNs is their **rapid time variability**. Consider an **optically thick sphere of radius R** that **simultaneously** (in its own rest frame) **brightens everywhere**; see Fig. 22. The **news of the change reaches a distant observer first from the nearest part** of the sphere after traveling a distance l_1 , and last from the edge or limb after traveling a distance l_2 . (The back of the sphere isn't seen.) Using

$$\ell_2 = \frac{\ell_1 + R}{\cos \theta} \simeq \ell_1 + R$$

Unified model of AGN

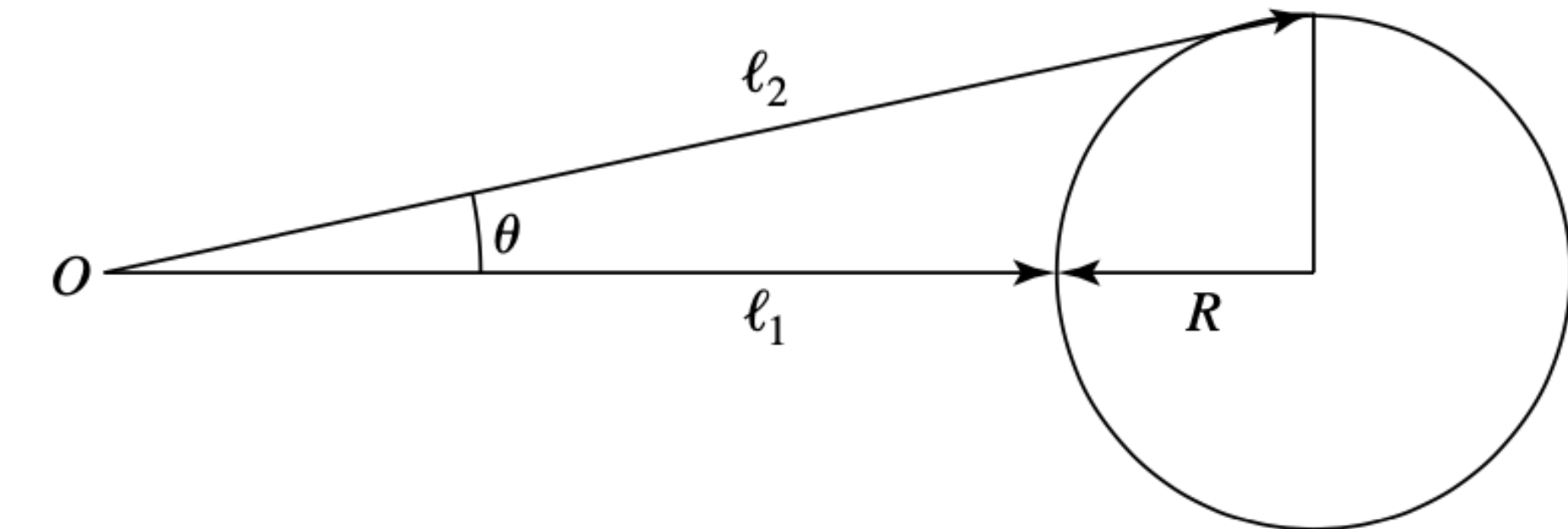


FIGURE 22 The brightening of a sphere as seen by a distant observer at point *O*.

for $R \ll l_1$ and $\cos \theta \approx 1$, the **light from the limb of the sphere must travel an additional distance of $l_2 - l_1 \approx R$** . The **brightening is thus smeared out over a time interval $\Delta t = R/c$** . In this way, **the rapidity of a luminosity change can be used to set an upper limit on the size of the object involved**. The high recessional speeds of quasars mean that **relativity also plays a role**. If the sphere described above were moving away from Earth with a velocity v , then its radius as determined on Earth would be

$$R = c\Delta t \sqrt{1 - \frac{v^2}{c^2}} = \frac{c\Delta t}{\gamma},$$

where γ is the Lorentz factor.

Unified model of AGN

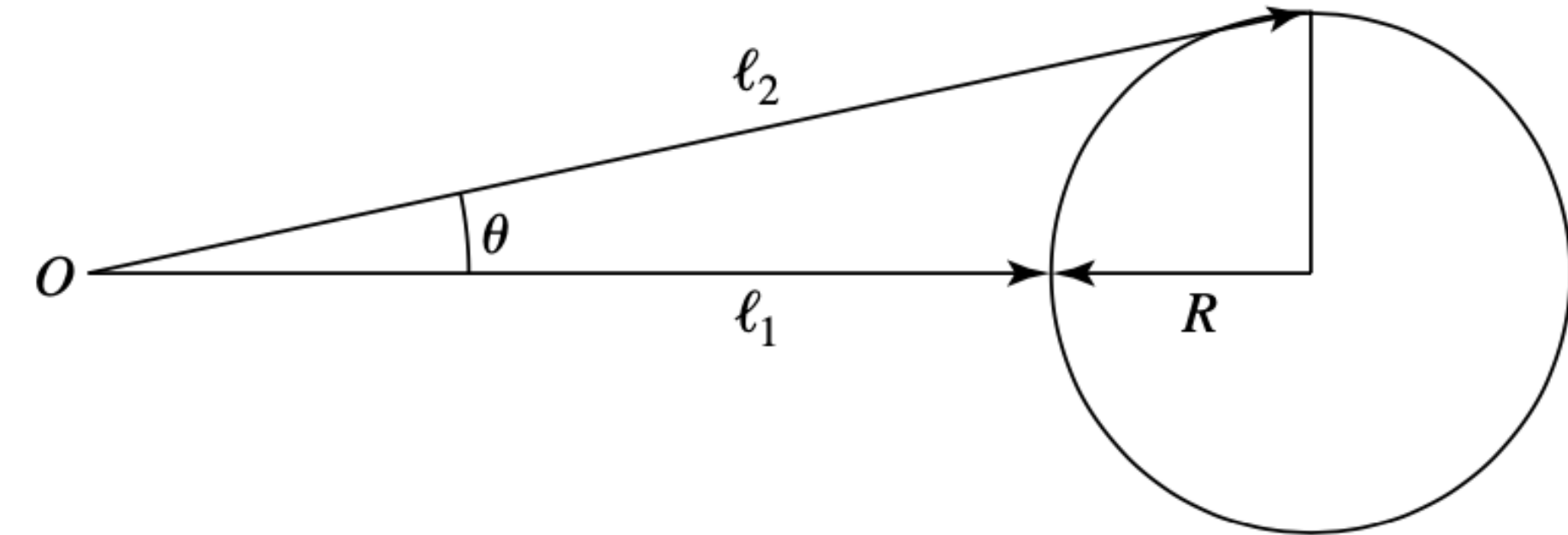


FIGURE 22 The brightening of a sphere as seen by a distant observer at point O .

Using $\Delta t = 1$ hr for a typical value, and taking $\gamma = 1$ for convenience, the radius of the emitting region is no more than

$$R \simeq \frac{c\Delta t}{\gamma} = 1.1 \times 10^{12} \text{ m} = 7.2 \text{ AU}.$$

Neptune is around ~ 30 AU, Saturn is at ~ 9 AU, and Jupiter is at ~ 5 AU from the Sun.

Considering that **AGNs are the most luminous objects known**, this is an **incredibly small size**. Whatever powers an active galactic nucleus would fit comfortably within our Solar System!

Unified model of AGN

The typical quasar luminosity of 5×10^{39} W is equivalent to **more than 360 Milky Way galaxies**. However, there is an **upper limit to the luminosity, L, of any spherically symmetric object that is in equilibrium**. It must be less than the **Eddington limit**, $L < L_{\text{Ed}}$, where,

$$L_{\text{Ed}} \simeq 1.5 \times 10^{31} \text{ W} \left(\frac{M}{M_{\odot}} \right).$$

For a luminosity of $L = 5 \times 10^{39}$ W, this provides a lower **limit for the mass**:

$$M > \frac{L}{1.5 \times 10^{31} \text{ W}} M_{\odot} = 3.3 \times 10^8 M_{\odot}.$$

Finding such a **large amount of mass in such a small space** is **clear evidence for a supermassive black hole**.

Unified model of AGN

The mass of a black hole with the radius R found is

$$M = \frac{Rc^2}{2G} = 3.7 \times 10^8 M_\odot.$$

The fact that these two mass estimates are of the **same order of magnitude** is enough to **support the idea** that supermassive black holes are involved in powering AGNs.

For the rest of this section, we will assume a value of $10^8 M_\odot$ for a typical mass, which corresponds to a Schwarzschild radius of $R_S \approx 3 \times 10^{11} \text{ m} \approx 2 \text{ AU} \approx 10^{-5} \text{ pc}$.

Accretion

The most efficient way of generating energy is by the **release of gravitational potential energy through mass accretion**. For matter falling onto the surface of a $1.4 M_{\odot}$ neutron star, **about 21% of the rest energy is released**.

However, dropping matter straight down onto a black hole is very *inefficient* because there is no surface for the mass to strike. Instead, according to an observer at a great distance, a freely falling mass would slow to a halt and then disappear as it approached the Schwarzschild radius, R_S . On the other hand, **as matter spirals in toward a black hole through an accretion disk, a substantial fraction of the rest energy can be released as viscosity converts kinetic energy into heat and radiation.**

For a **nonrotating black hole**, the smallest stable circular orbit for a massive particle (and therefore the **inner edge of an accretion disk**) is at $r = 3R_S$. At this location, calculations show that the gravitational binding energy is **5.72% of the particle's rest-mass energy**, so mass spiraling down through an accretion disk **would release** this much energy.

The situation is even more favorable for a **rotating black hole** because the **event horizon is at a smaller r** . For the most rapidly rotating black hole possible, both the event horizon and the smallest stable prograde orbit are at $r = 0.5R_S$ (the smallest stable retrograde orbit is at $4.5R_S$). The gravitational binding energy in this case of maximal rotation is calculated to be **42.3% of a particle's rest mass**.

Accretion

The **accretion luminosity** generated by a mass accretion rate, \dot{M} , through the disk may be written as

$$L_{\text{disk}} = \eta \dot{M} c^2,$$

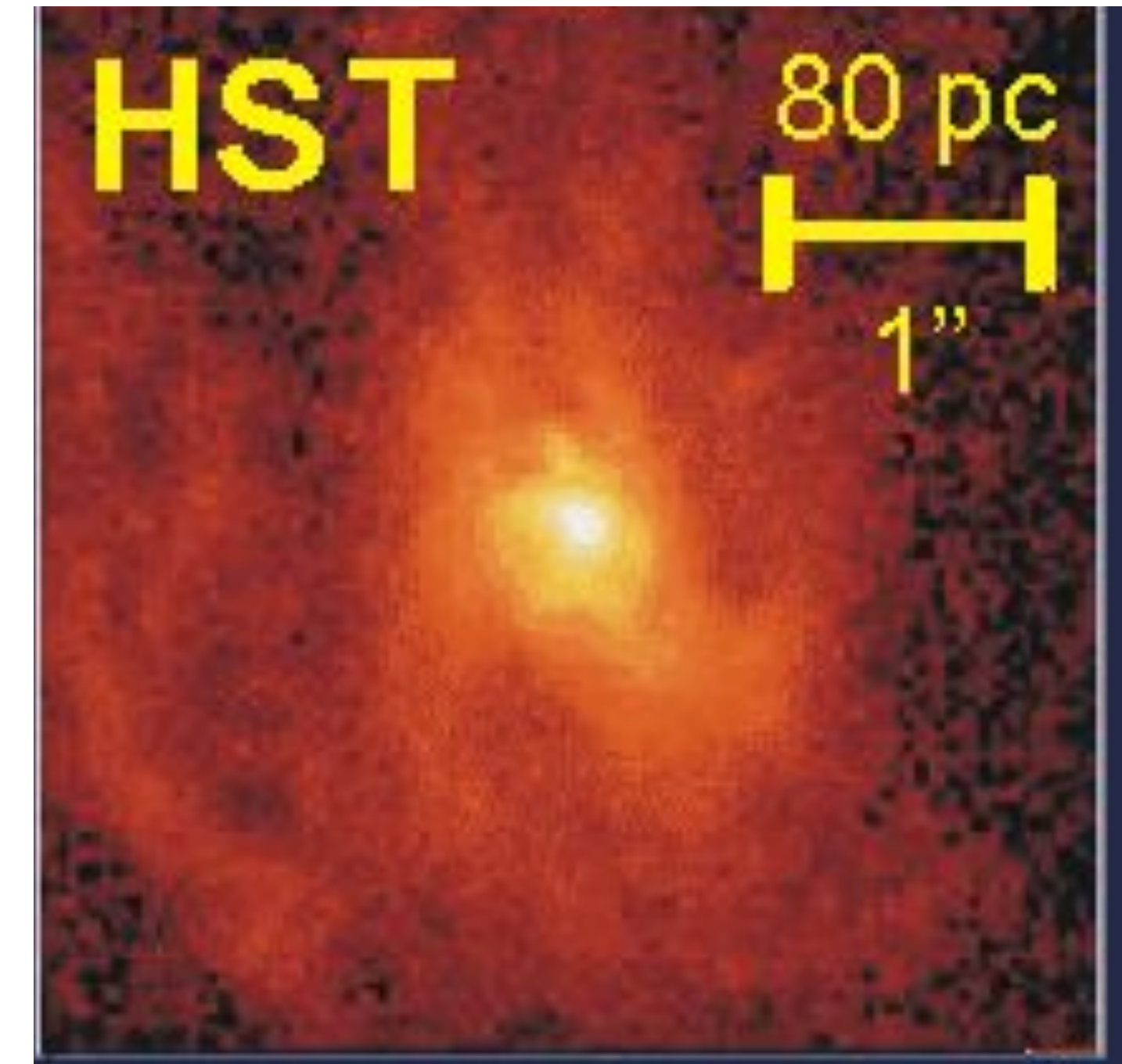
where η is the efficiency of the process, $0.0572 \leq \eta \leq 0.423$. (For comparison, the efficiencies for accretion onto a $0.85 M_\odot$ white dwarf and a $1.4 M_\odot$ neutron star are $\eta = 1.9 \times 10^{-4}$ and 0.21, respectively.)

The **accretion of matter** through a disk around a **rapidly rotating black hole** is an **extremely efficient** way of producing large amounts of energy. Furthermore, the smallest stable prograde orbit lies inside the ergosphere of a rapidly rotating black hole, and frame dragging guarantees that the accreting matter will rotate along with the black hole.

For these reasons, an accretion disk around a supermassive black hole is an essential ingredient of a unified model of AGNs. -> need the energy to produce the brightness of the AGN

Accretion

The Figure shows the spiral-shaped disk of gas that lies at the center of M87. The inner edge of the disk is rotating with a speed of about 550 km s^{-1} , causing the light from the lower right-hand edge of the disk to be blueshifted (approaching), while the light from the upper-right is redshifted (receding). The central supermassive black hole is calculated to have a mass of about $3 \times 10^9 \text{ M}_\odot$.



The inner regions of **accretion disks around white dwarfs and neutron stars are bright at ultraviolet and X-ray wavelengths**, respectively.

It might be expected that an accretion disk around a supermassive black hole would be a source of photons of even higher energies, but this is not the case. Because they are supported by degeneracy pressure, white dwarfs and neutron stars obey the mass–volume relation, which states that these stars **become smaller with increasing mass**. Therefore, the accretion disks around more massive white dwarfs and neutron stars penetrate deeper into their gravitational potential wells. The **Schwarzschild radius, however, increases with increasing mass**, and so the characteristic **disk temperature, T_{disk} , decreases as the mass of the black hole increases**.

Accretion

To see this, we will assume a rapidly rotating black hole and adopt $R=0.5R_S = GM/c^2$ for the location of the inner edge of the accretion disk. The characteristic disk temperature becomes

$$T_{\text{disk}} = \left(\frac{3c^6 \dot{M}}{8\pi\sigma G^2 M^2} \right)^{1/4}.$$

For a disk radiating at a **fraction f_{Ed} of the Eddington limit**,

$$f_{\text{Ed}} \equiv L_{\text{disk}}/L_{\text{Ed}}.$$

$$\eta \dot{M} c^2 = f_{\text{Ed}} \frac{4\pi G c}{\bar{\kappa}} M, \quad \dot{M} = \frac{f_{\text{Ed}}}{\eta} \frac{4\pi G}{\bar{\kappa} c} M.$$

Substituting this expression into T_{disk} shows that

$$T_{\text{disk}} = \left(\frac{3c^5 f_{\text{Ed}}}{2\bar{\kappa}\sigma GM\eta} \right)^{1/4},$$

and so for the disk temperature, $T_{\text{disk}} \propto M^{-1/4}$.

Accretion

Example 2.1. Consider an **accretion disk around a rapidly rotating supermassive black hole of $10^8 M_\odot$.**

The value of f_{Ed} is probably close to 1 for luminous quasars and roughly between 0.01 and 0.1 for Seyfert galaxies. In this example, let the disk luminosity be equal to the Eddington limit ($f_{\text{Ed}} = 1$), so $L = 1.5 \times 10^{39} \text{ W}$. Also, we will adopt $\eta = 0.1$ as a representative accretion efficiency.

The mass accretion rate required to maintain the disk luminosity is

$$\dot{M} = \frac{f_{\text{Ed}}}{\eta} \frac{4\pi G}{\bar{\kappa}c} M = 1.64 \times 10^{23} \text{ kg s}^{-1} = 2.60 M_\odot \text{ yr}^{-1}.$$

Luminous quasars must be fed at a rate of around 1 to $10 M_\odot \text{ yr}^{-1}$. Less luminous AGNs may have correspondingly smaller appetites.

Accretion

The characteristic disk temperature is

$$T_{\text{disk}} = \left(\frac{3c^5 f_{\text{Ed}}}{2\bar{\kappa}\sigma GM\eta} \right)^{1/4} = 7.30 \times 10^5 \text{ K},$$

Where $X = 0.7$ has been used for the **opacity** due to electron scattering. According to Wien's law, the spectrum of a blackbody with this **temperature peaks** at a wavelength of 39.7 nm, **in the extreme ultraviolet** region of the electromagnetic spectrum.

Although this expression for T_{disk} is at best a **rough estimate** of the characteristic disk temperature, temperatures of several hundred thousand kelvins agree with the results of more realistic disk calculations.

It is thought that the **big blue bump observed** in the spectra of quasars is the thermal **signature of an underlying accretion disk**.

However, **the accretion disk alone cannot account for the wide continuum that is actually observed**.

Accretion

A detailed model of the accretion disk around a supermassive black hole is difficult to derive because **the high luminosities involved must have a significant effect on the disk's structure.**

Theoretical calculations indicate that the structure of the accretion disk depends on f_{Ed} . Several possible structures have been identified.

- If $f_{Ed} < 0.01$, then the **density of the disk is too small for efficient cooling**. The energy generated by the disk's viscosity (internal friction) **cannot be radiated away** efficiently, and the **disk puffs up** into an **ion torus** that is supported by the pressure of the hot ions. Part or all of the disk would then resemble a doughnut around the central black hole.
- Values of $0.01 < f_{Ed} < 0.1$ or so imply a **geometrically thin disk** for close binary systems (by definition, at any radial distance r in a thin disk, the vertical height $h \ll r$).
- As the value of L_{disk} becomes **super-Eddington** ($f_{Ed} > 1$), the **radiation pressure that is generated balances the force of gravity** and the photons are capable of supporting the matter in an **inflated radiation torus**.

Accretion

One scenario involves a composite disk that has three regions, as shown in Fig. 23.

- Within about $10^3 R_S$ of the center, **radiation pressure exceeds the gas pressure, resulting in a thick, hot disk**. This is the probable origin of the **big blue bump** in the continuous spectrum.

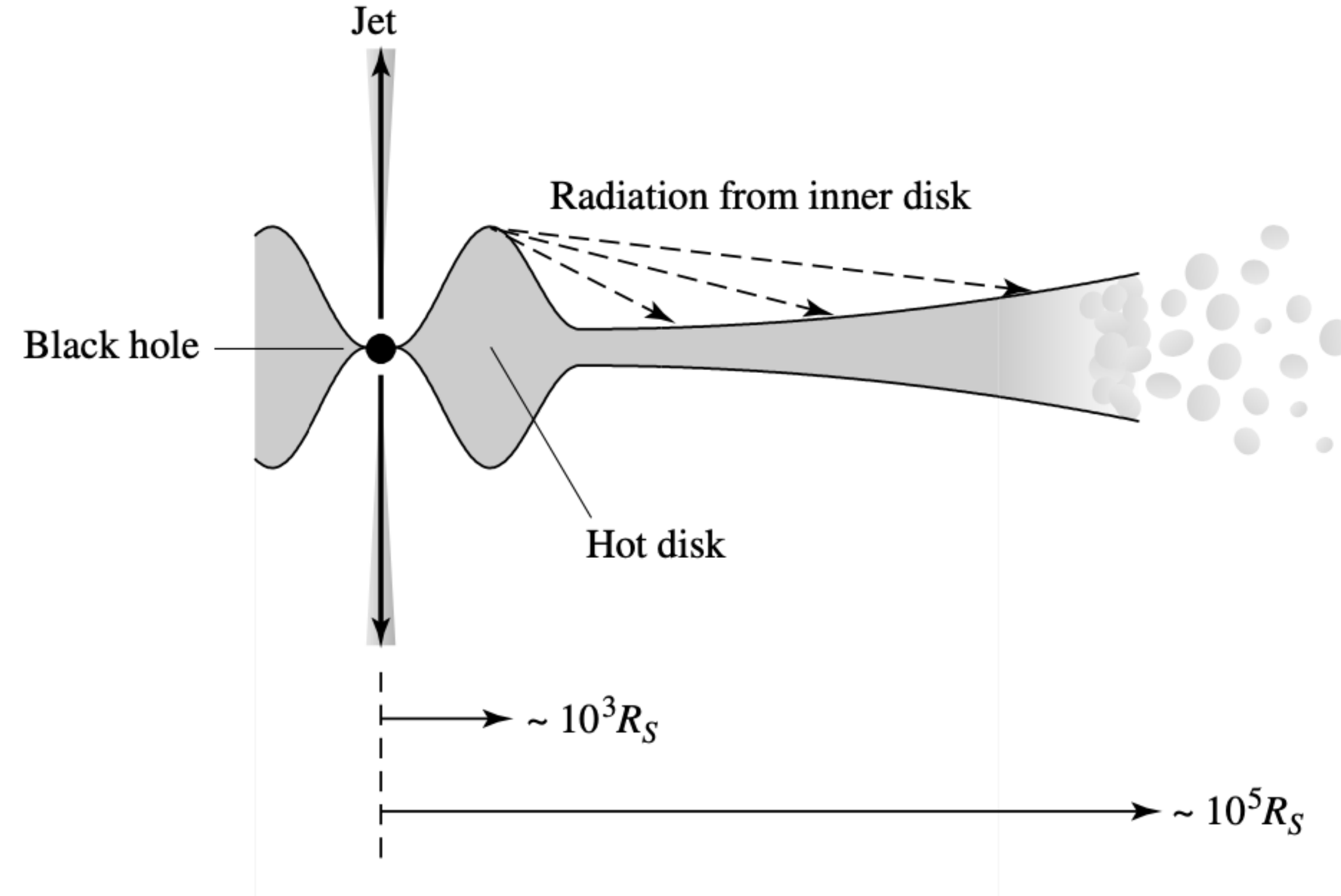


FIGURE 23 A schematic structure of the accretion disk in an AGN. The radial direction is not drawn to scale.

- Exterior to this, reaching out to some $10^5 R_S$ (≈ 1 pc for $M = 10^8 M_\odot$), is a **thin disk** that is supported by **gas pressure**. This part of the disk **flares outward**, becoming **thicker with increasing radius**. The concave surface of the outer disk means that it can be **irradiated by the central source or the thick, hot portion of the inner disk**, resulting in a wind flowing outward from the disk.
- Finally, beyond about $10^5 R_S$, the **thick disk breaks up into numerous small clouds**.

Some problems with this picture remain. For example, the values of f_{Ed} quoted above for **Seyferts appear to be incompatible with models of thick disks**.

AGN Spectra

Synchrotron radiation is produced when relativistic charged particles, such as electrons, spiral around magnetic field lines.

(For objects other than blazars, the situation is more complicated. The **big blue bump** observed in the continua of other types of AGNs is believed to be **thermal radiation**. In addition, **dust emission** plays an important role in the **infrared**.)

With a wide range of photon energies available for ionizing atoms, **synchrotron radiation can account for the variety of ionization states observed in the emission line spectra** of AGNs. For example, a number of ionization states have been seen for forbidden lines, including [O I] and [Fe X]. Furthermore, **synchrotron radiation can be up to 70% linearly polarized**, in agreement with the high degrees of polarization observed for some AGNs.

Relativistic outflow

Black holes should be essentially electrically neutral, since any net charge acquired by a black hole would be rapidly canceled as it attracted charge of the opposite sign.

However, the ionized disk material is highly conducting, so there can be a **magnetic field that is generated by the accretion disk** as the disk orbits the black hole. The **varying magnetic field near the surface of the disk** may induce a large electric field that is capable of **accelerating charged particles away from the disk**. As the particles move outward, they are **accelerated to relativistic speeds** while they **spiral around the magnetic field lines that rotate with the disk**. Because the field lines are anchored to the conducting disk, the particle energy ultimately comes at the expense of the accretion energy.

Relativistic outflow

There is another source of energy that taps the rotational energy of the black hole itself. Calculations show that the rotating black hole can be thought of as a spinning conductor in a magnetic field; see Fig. 24. Just as the motion of a conducting wire through a magnetic field will produce an electromotive force between its ends, **the rotation of a black hole in a magnetic field will produce a potential difference between its poles and its equator.**

The effective resistance of the rotating black hole between its poles and equator is about 30Ω . In this picture, the black hole acts like an immense battery connected to a 30Ω resistor. Power is extracted from the black hole's rotational energy, just as if a current of charged particles were flowing through the resistor in response to the voltage difference. As a result, the black hole's rate of spin is reduced.

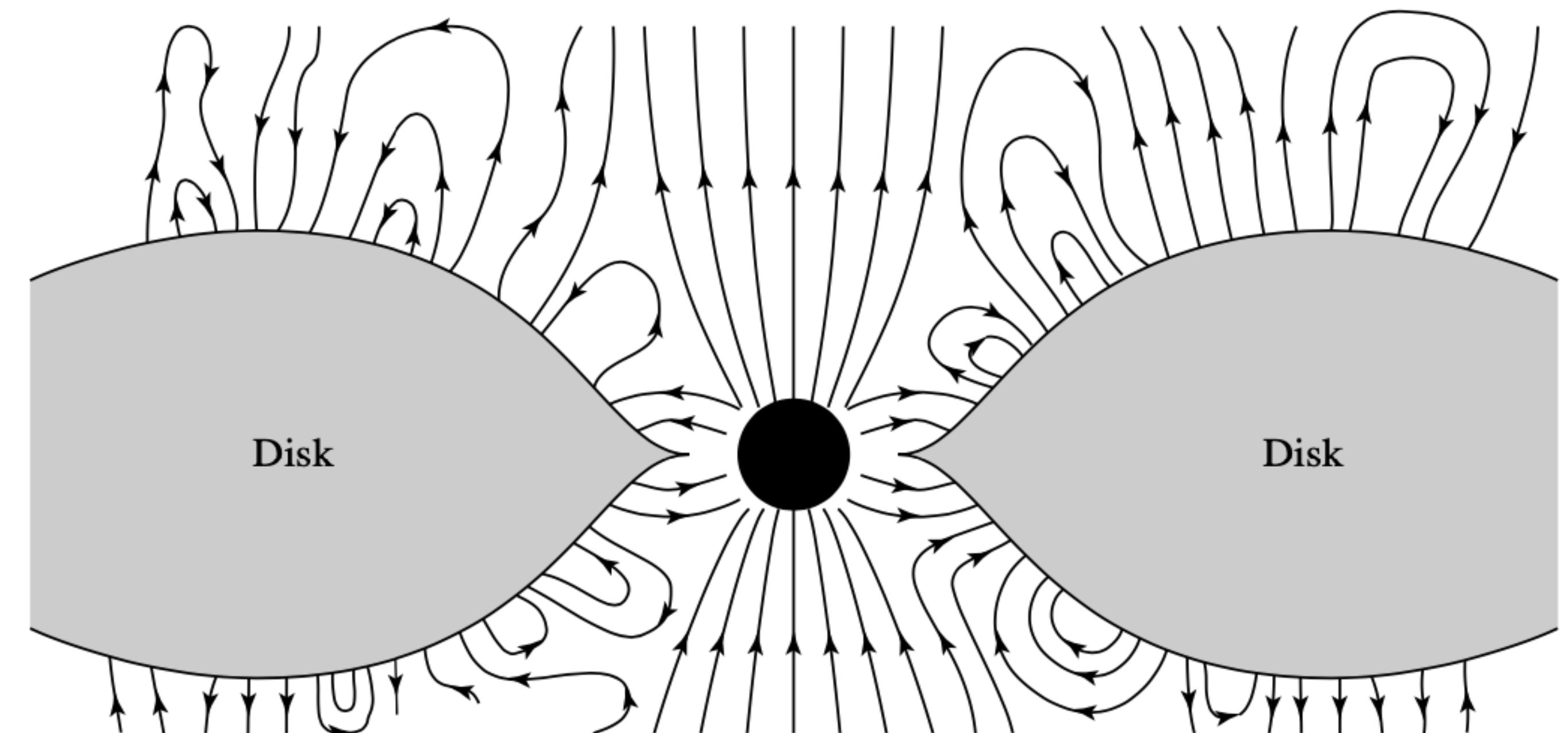


FIGURE 24

An accretion disk and its magnetic field orbiting a rotating black hole.

Relativistic outflow

The power generated by the **Blandford–Znajek mechanism** is approximately

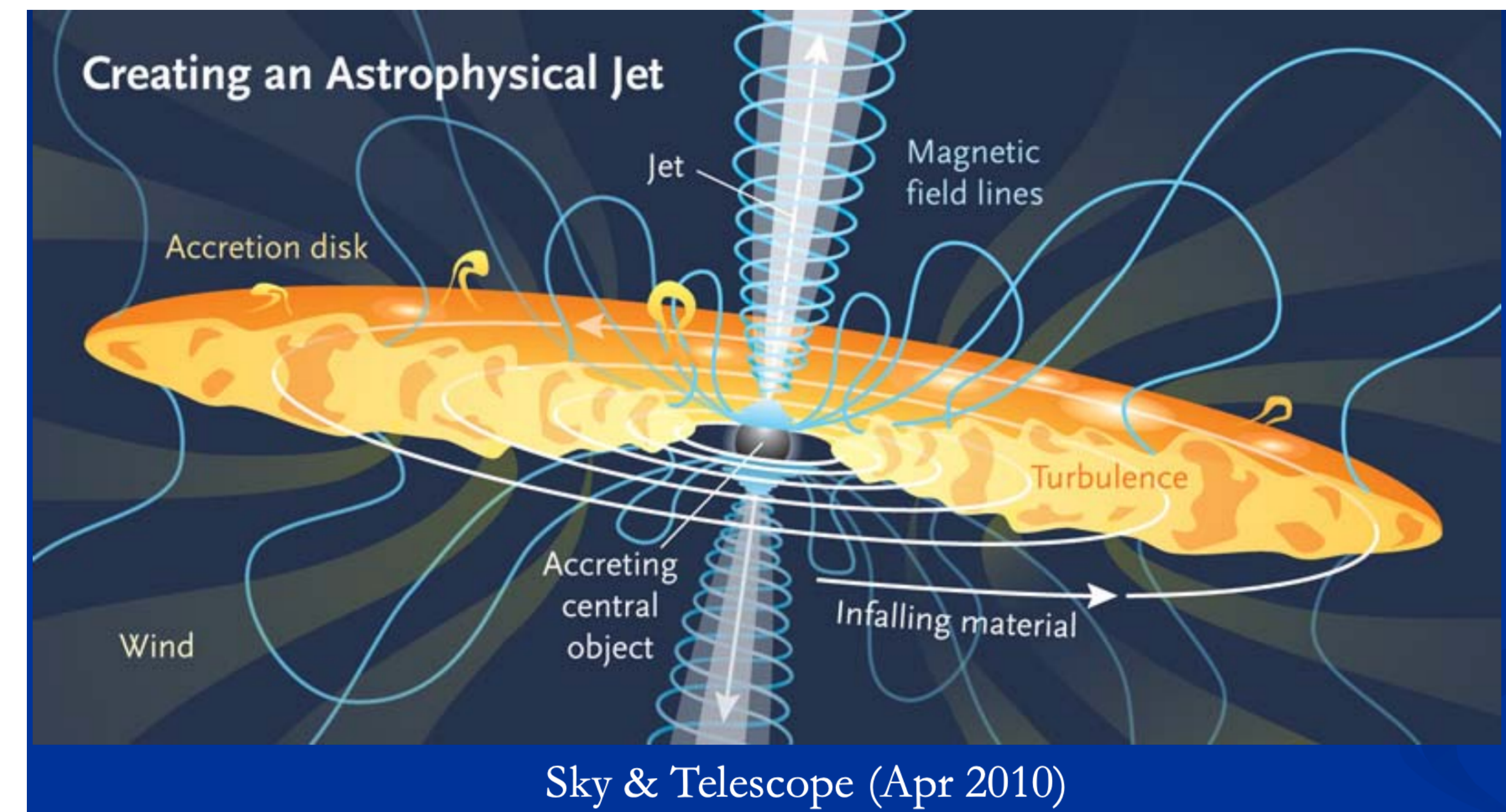
for a $10^8 M_\odot$ black hole with $R_S = 3 \times 10^{11}$ m and a magnetic field of 1 T. The energy is in the form of electromagnetic radiation and a flow of relativistic pairs of electrons and positrons.

Up to 9.2% of the rest energy of a maximally rotating black hole may be extracted in this manner.

Relativistically accelerated electrons in the magnetic field => Synchrotron radiation

The two processes just described appear capable of producing a relativistic outflow of charged particles, although the mechanism is still uncertain.

$$P \simeq \frac{4\pi}{\mu_0} B^2 R_S^2 c \\ = 2.7 \times 10^{38} \text{ W} = 7.1 \times 10^{11} L_\odot$$



Generating X-rays

AGNs can be very bright in X-rays, and several mechanisms are usually invoked to explain the excess over that produced directly by synchrotron radiation. The high-frequency end of the **accretion disk** spectrum may be sufficient to **account for the soft (low-energy) X-rays**. Lower-energy **photons** from other sources **may also be scattered to much higher energies** by collisions with relativistic electrons. As the name suggests, this **inverse Compton scattering** is the reverse of the Compton scattering process.

In addition, **inverse Compton scattering may produce the gamma rays** coming from the quasar 3C 273. **Thermal bremsstrahlung**, the mechanism that produces the **X-ray emission** observed in clusters of galaxies, has a characteristic spectrum that could also be consistent with observations of X-rays from AGNs.

Line emission

The characteristic broad emission lines (when present) and narrow emission lines of AGNs are the result of **photoionization by the continuum radiation**.

All of the **broad lines** arise from **permitted atomic transitions**, but none of them involve the **forbidden transitions seen in some narrow lines**. The **broad H α and H β lines vary on timescales of a month or less**, while the narrow lines seem to vary little, if at all.

This evidence, along with the discovery that Seyfert 2 galaxies may harbor Seyfert 1 nuclei that are hidden from direct view by some obscuring material, indicates that the **broad and narrow lines in the spectra of AGNs originate in different regions under different conditions**.

Broad-line emission

The broad emission lines observed in the spectrum of many AGNs are formed in a **broad-line region** that is **relatively close to the center**.

A study of the **Seyfert** galaxy NGC 4151 revealed that **when the intensity of the continuum radiation varied, most of the broad emission lines responded very quickly**, within a month or less and perhaps as quickly as one week.

Light can travel a distance of nearly 10^{15} m in 30 days, so this provides a rough estimate of the radius of the broad-line regions for Seyferts and BLRGs. The variation of the lines in quasars takes place more slowly, so their broad-line regions may be larger by a factor of four or so. A study of the broad Fe II emission lines that are usually present indicates that the **temperature in the broad-line region is $\sim 10^4$ K**. Other lines indicate that the **number density of electrons probably lies between 10^{15} m $^{-3}$ and 10^{16} m $^{-3}$** . Forbidden lines will not be seen with large number densities such as these because of the **frequent collisions between the atoms**. Atoms and ions with electrons in the long-lived metastable states that give rise to forbidden lines are deexcited by collisions before downward radiative transitions can occur. As a result, the **forbidden lines are much weaker than the permitted lines**.

Broad-line emission

There is widespread agreement that the **broad-line region must be clumpy**, containing partially ionized clouds of gas, rather than being homogenous. The optically thick clouds that actually produce the emission lines fill only about 1% of the available volume and probably have a flattened distribution. These regions of high density may be surrounded by a rarefied, high-temperature medium that prevents the clouds from dispersing.

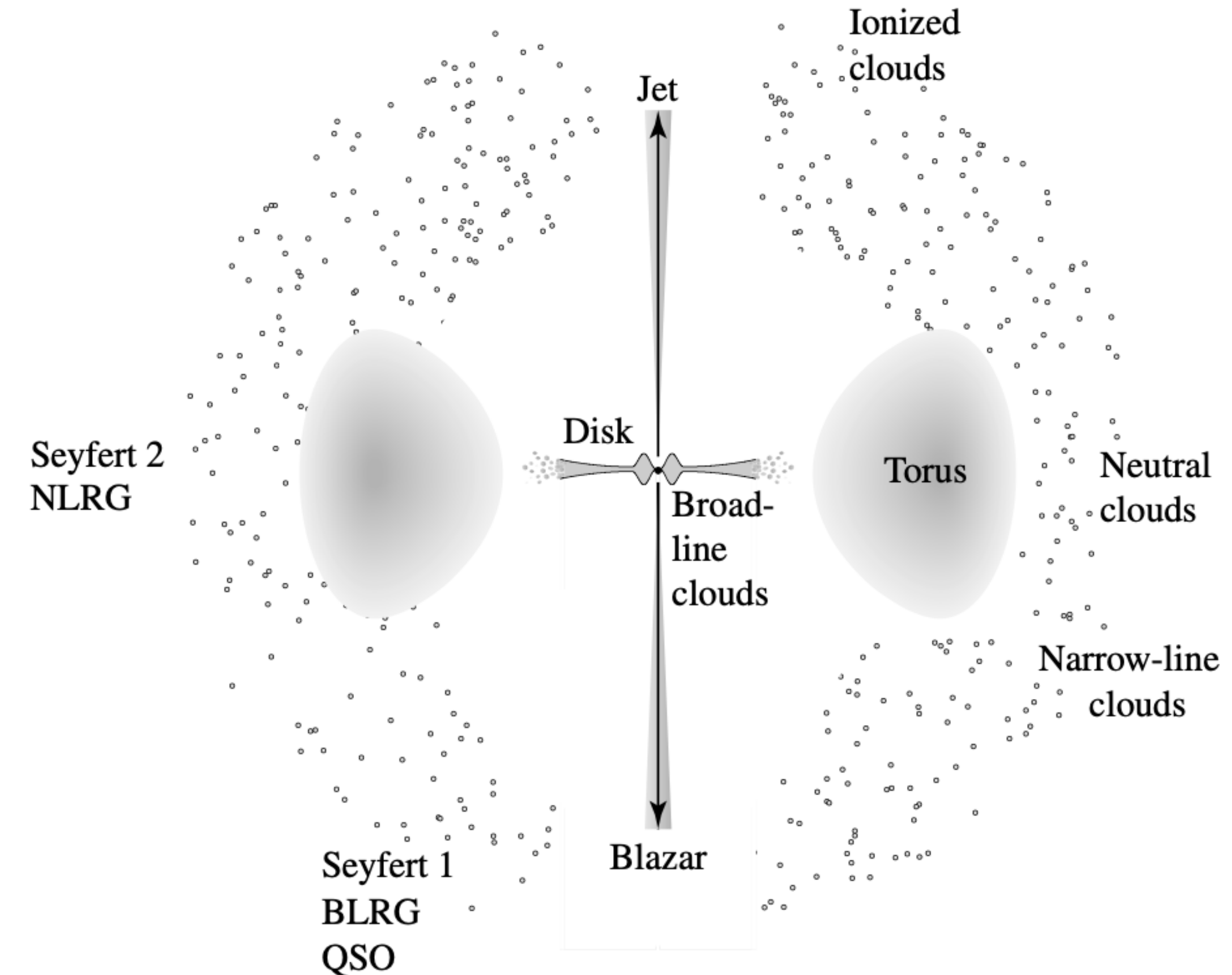


FIGURE 25 A sketch of a unified model of an active galactic nucleus. The jets would be present in a radio-loud AGN. A typical observer's point of view is indicated for AGNs of various types.

According to the unified model, the various types of observed AGN phenomena (see Table 1) derive from different viewing angles of the central engine and surrounding environment. The unified model postulates that a large, **optically thick torus of gas and dust surrounds the clouds of the broad-line region**. This is presumably what conceals the broad-line region and the central source from direct view when observing a Seyfert 2 galaxy; see Fig. 25.

Broad-line emission

In this case, the continuum and emission lines must reach the observer indirectly by reflected light, which explains why the continuum of Seyfert 2s is much fainter than the continuum of Seyfert 1s. **Overall, the light received directly from the central nucleus makes Seyfert 1 galaxies generally brighter than Seyfert 2s.** The torus is also thought to be opaque to soft X-rays because the X-rays observed for Seyfert 2s are hard (with energies above approximately 5 keV).

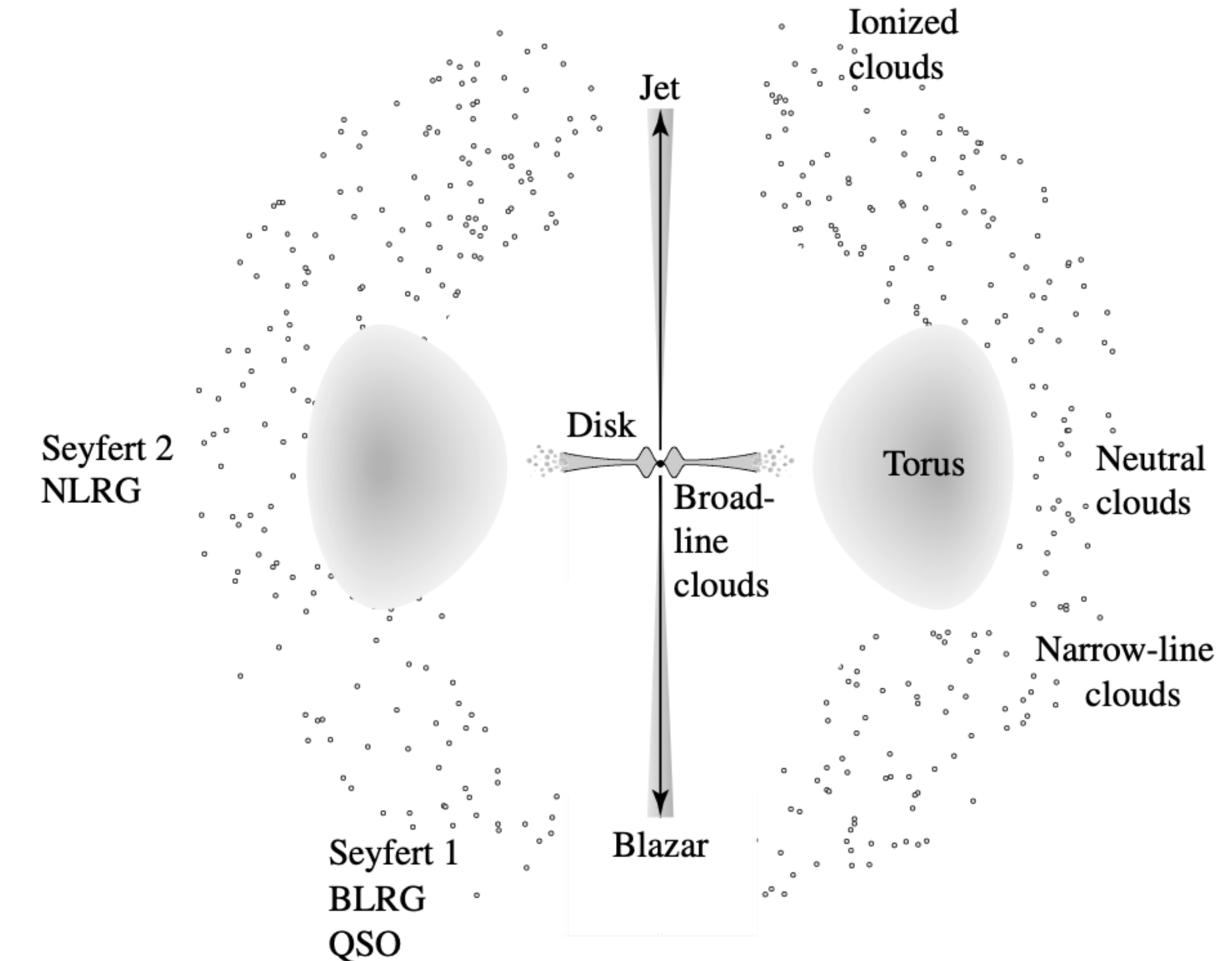


FIGURE 25 A sketch of a unified model of an active galactic nucleus. The jets would be present in a radio-loud AGN. A typical observer's point of view is indicated for AGNs of various types.

Broad-line emission

The broad emission lines also indicate that the clouds orbit the central supermassive black hole. In fact, taking the 5000 km s^{-1} width of the lines to be an orbital velocity and using $r = 10^{15} \text{ m}$ as an orbital radius provides an estimate of the **central mass**.

$$M_{\text{bh}} = \frac{rv^2}{G} = 1.9 \times 10^8 M_{\odot},$$

which is consistent with previous mass estimates.

A second technique for determining the masses of the central black holes of AGNs in broad-line regions is based on measuring the **lag time between changes in brightness of the continuum and emission lines**. This **reverberation mapping** technique combines the measured time delay, τ , with the root-mean-square width of the emission line, σ_{line} , giving a mass estimate of

$$M_{\text{bh}} = \frac{fc\tau\sigma_{\text{line}}^2}{G},$$

where c is the speed of light and f is a factor that depends on the structure, kinematics, and orientation of the broad-line region.

Broad-line emission

By comparison with other black hole–spheroid relations, such as the **mass–velocity dispersion relation for a sample of resolved galactic centers**, the scaling factor in the equation is found to have the value $f \approx 5.5$.

The reverberation mapping method requires long-term observations to determine the lag times, and high spectral resolution, but it does not require spatially resolving the central region of the host galaxy. Thus, the reverberation technique holds great promise for measuring black hole masses in AGNs that are at high z .

Figure 26 shows the results of a study of AGN broad-line emission regions.

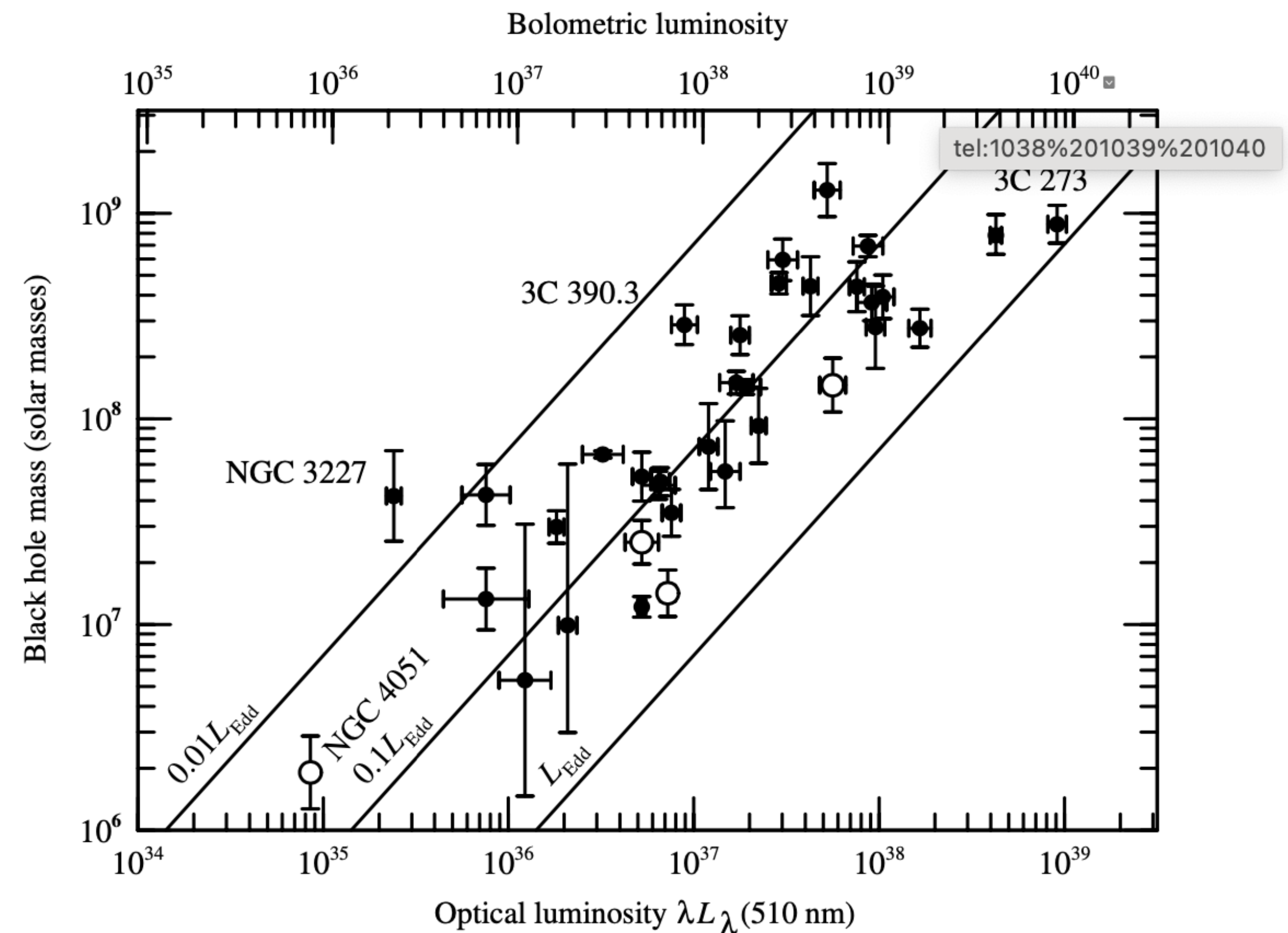


FIGURE 26 The masses of the supermassive black holes in AGNs as a function of their luminosities. The solid diagonal lines represent lines of constant fractions of the Eddington luminosity. The masses were determined by the reverberation mapping technique. The bolometric luminosities are given on the top axis, and the optical luminosities (centered at 510 nm) are given on the bottom axis. (Figure courtesy of Bradley Peterson.)

Narrow-line emission

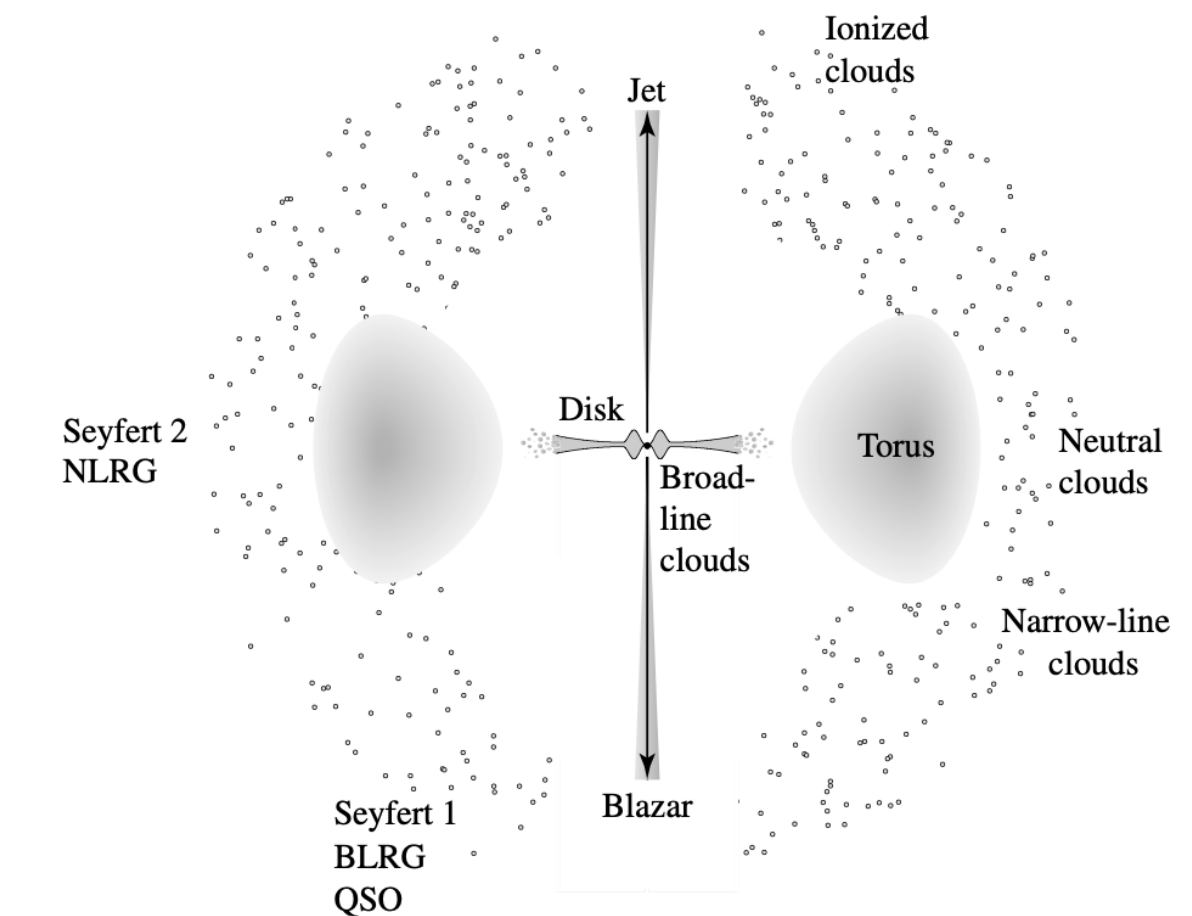


FIGURE 25 A sketch of a unified model of an active galactic nucleus. The jets would be present in a radio-loud AGN. A typical observer's point of view is indicated for AGNs of various types.

Outside the opaque torus is the **narrow-line region** where the narrow emission lines originate. The number density of electrons in the narrow-line region is only about 10^{10} m^{-3} , comparable to the values found in **planetary nebulae and dense H II regions**.

The narrow-line region contains more mass than the broad-line region, and both **permitted and forbidden lines** can be formed in such an environment.

They reveal a **temperature of approximately 10^4 K** . Like the broad-line region, the region that generates the narrow-line spectrum is **clumpy**.

It is probably composed of a **more or less spherical distribution of clouds**. The **clouds that are far enough above or below the plane** of the obscuring torus can be illuminated and **photoionized by the continuum radiation** from the center. Other clouds have their lines of sight to the central source blocked by the opaque torus, and so they remain neutral.

Narrow-line emission

In fact, if the narrow-line region **can be treated as a clumpy H II region**, then the Strömgren radius can be used to estimate the fraction of the narrow-line region that is occupied by clouds. If the clouds occupy a fraction ϵ (referred to as the **filling factor**) of the volume of the narrow-line region, it can be modified to produce an estimate of the radius of that region,

$$r_{\text{NLR}} \approx \left(\frac{3N}{4\pi\alpha_{\text{qm}}\epsilon} \right)^{1/3} \frac{1}{n_e^{2/3}}.$$

In this case N is the number of photons per second produced by the central source of the AGN that have enough energy to ionize hydrogen from the ground state, and **α_{qm} is a quantum-mechanical recombination coefficient**.

Narrow-line emission

Example 2.2. To estimate the filling factor of the narrow-line region, we will assume an AGN luminosity of $L = 5 \times 10^{39}$ W. The continuum includes photons with a wide range of energies. We will assume that the monochromatic energy flux (Eq. 1) obeys a power law with a spectral index of $\alpha = 1$. Recalling Example 1, the flux is related to the luminosity:

$$L = 4\pi d^2 \int_{\nu_1}^{\nu_2} F_\nu d\nu = \int_{\nu_1}^{\nu_2} C\nu^{-1} d\nu$$

with $\nu_1 = 10^{10}$ Hz and $\nu_2 = 10^{25}$ Hz for the range of frequencies of the continuous spectrum, and C is a constant to be determined. Evaluating the integral and solving for C gives

$$C = \frac{L}{\ln(\nu_2/\nu_1)} = \frac{L}{\ln 10^{15}} = 0.029L.$$

Narrow-line emission

We are now ready to find N , the number of photons emitted per second with an energy $E_H > 13.6 \text{ eV}$, or a frequency $\nu_H > 3.29 \times 10^{15} \text{ Hz}$, **required to ionize hydrogen** from the ground state. Dividing the monochromatic energy flux by the energy per photon, $E_{\text{photon}} = h\nu$, results in

$$N = \int_{\nu_H}^{\nu_2} \frac{C\nu^{-1}}{h\nu} d\nu = \int_{\nu_H}^{\nu_2} \frac{0.029L}{h\nu^2} d\nu \simeq \frac{0.029L}{h\nu_H} = 6.64 \times 10^{55} \text{ s}^{-1},$$

where $\nu_2 \gg \nu_H$.

Observations of the nearest Seyfert 2 galaxies show narrow-line regions with diameters between roughly 100 and 1000 pc. If we let $r_{\text{NLR}} = 200 \text{ pc}$, $n_e = 10^{10} \text{ m}^{-3}$, and $\alpha_{\text{qm}} = 3.1 \times 10^{-19} \text{ m}^3 \text{ s}^{-1}$, the filling factor of the narrow-line region is approximately

$$\epsilon \approx \frac{3N}{4\pi\alpha_{\text{qm}}} \frac{1}{n_e^2 r_{\text{NLR}}^3} = 2.2 \times 10^{-2}.$$

Thus clouds occupy roughly 2% of the volume of the narrow-line region.

Narrow-line emission

The profiles of the **narrow emission lines** seen in Seyfert 2s often have **extended blue wings**, indicating that the **clouds are moving toward us** relative to the galactic nucleus. This is usually **interpreted as a radial flow of the clouds away from the center**. The light from the clouds moving away from us on the far side of the AGN is presumably diminished by extinction.

An outward flow of clouds in the region that produces narrow emission lines **could be driven by a combination of radiation pressure and a wind coming from the accretion disk**, or the outflow could be **associated with the material in radio jets**.

Figure 27 shows an image obtained by the Hubble Space Telescope of the narrow-line region for the **Seyfert 1 galaxy, NGC 4151**.

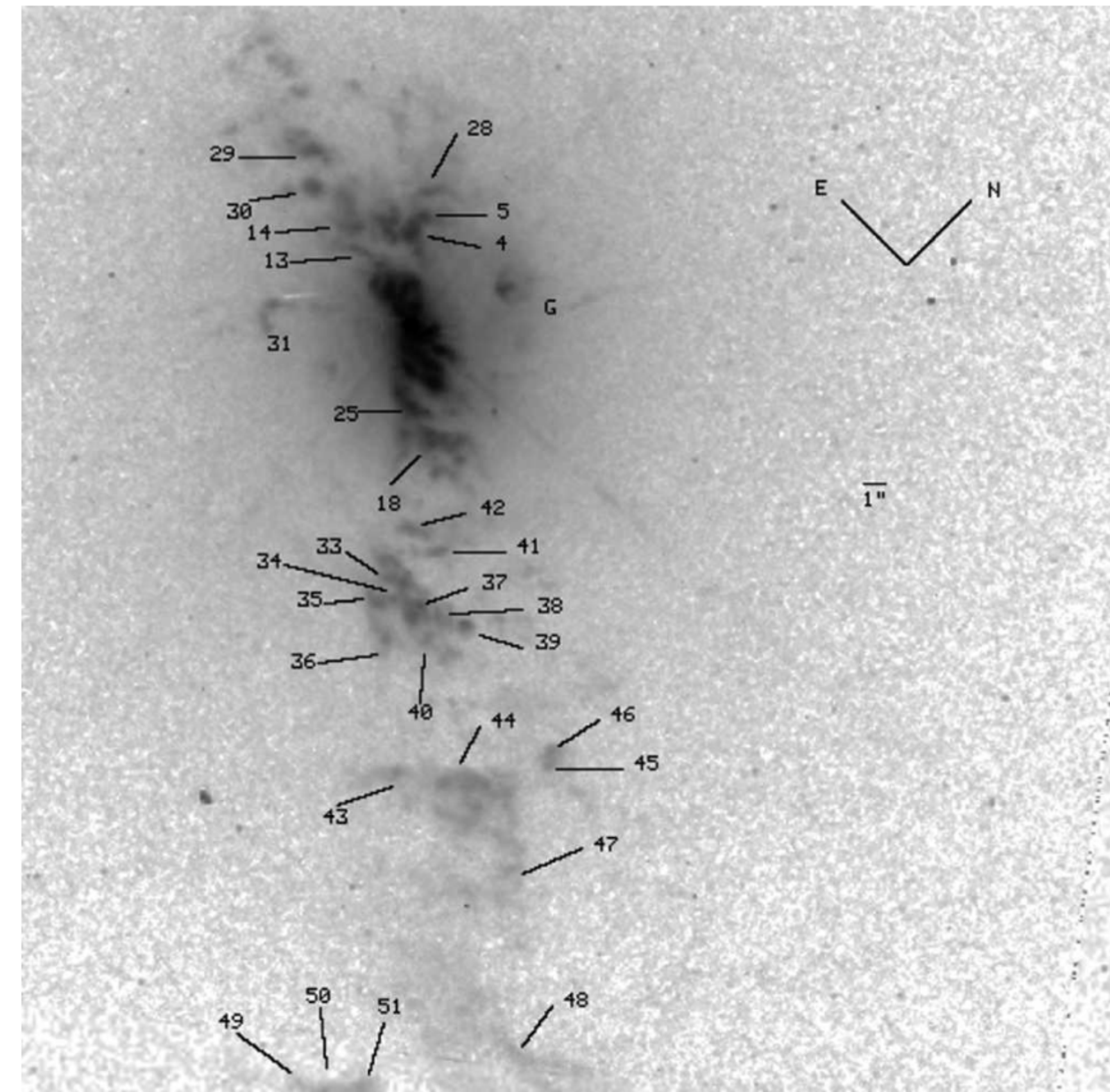


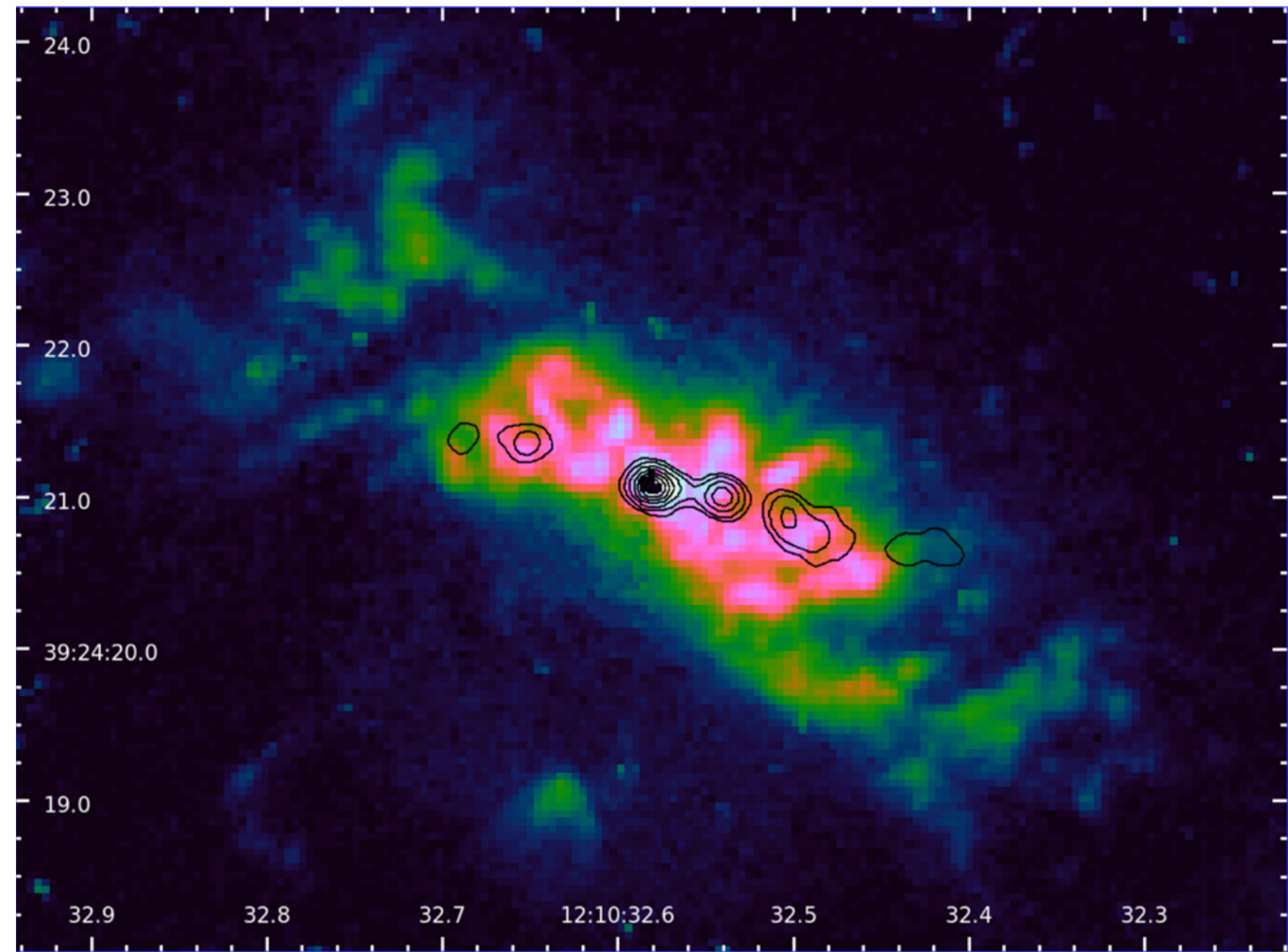
FIGURE 27 An HST image of the narrow-line region of the Seyfert 1 galaxy, NGC 4151. Numerous clouds are evident in a biconical distribution. The clouds to the southwest are approaching the observer relative to the nucleus, and the clouds to the northeast have recessional velocities. There is some evidence that the clouds may be associated with the galaxy's radio jets. An angular scale of 1" is indicated on the image; at the distance to NGC 4151, 1" corresponds to a projected linear distance of 63 pc. The labels correspond to clouds identified in the paper. (Figure from Kaiser et al., *Ap. J.*, 528, 260, 2000.)

Narrow-line emission

Distinct emission clouds are clearly evident in this high-resolution image.

It is also evident that the optical emission falls within **two conical distributions** extending to the northeast and the southwest of the center of the galaxy.

When a **radio map** is overlaid on the image, the radio emission also falls along the **same axis** as the biconical optical emission.

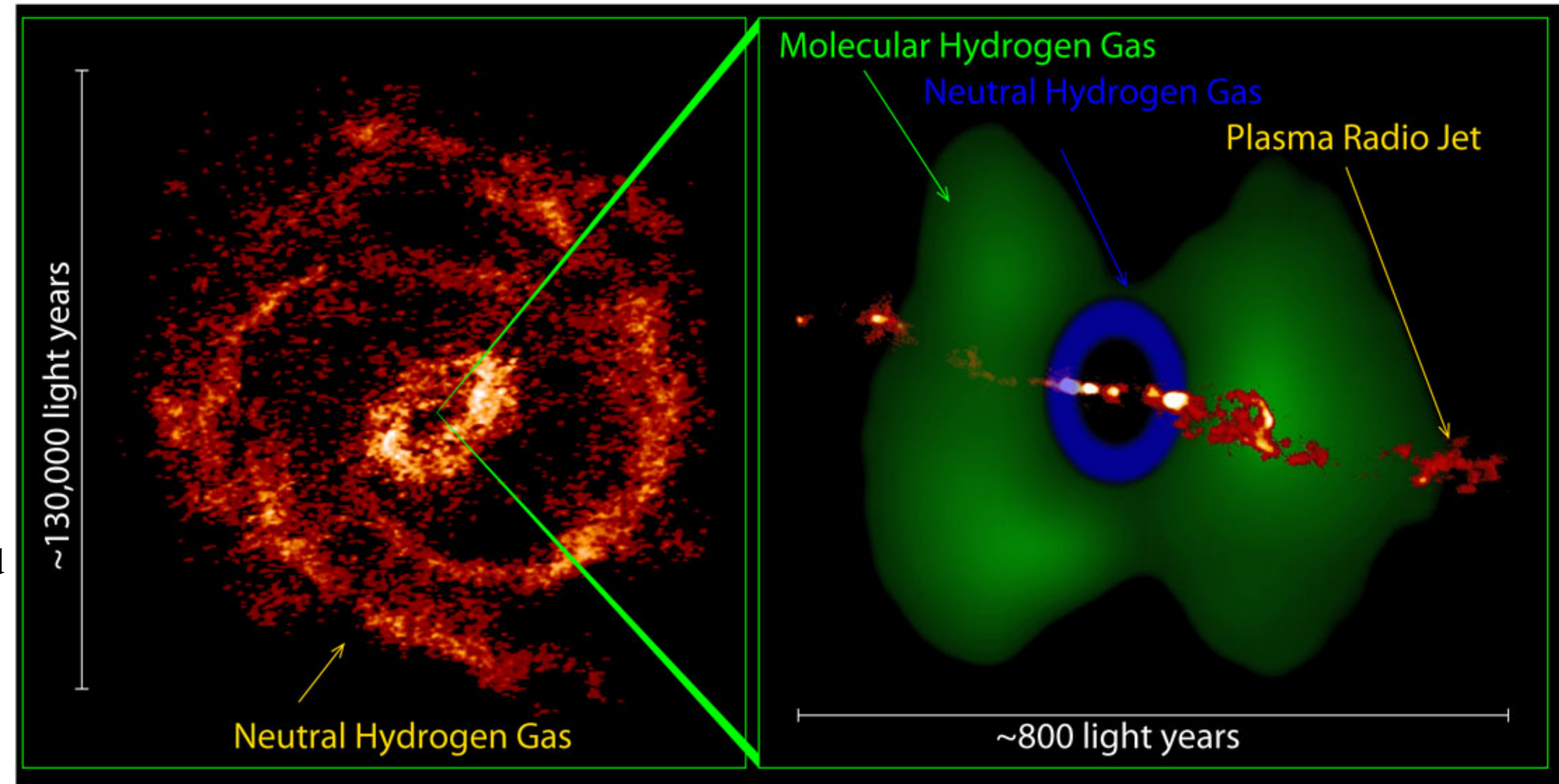


Williams et al. 2017, HST emission line images of NGC 4151 for [O III]. The full resolution eMERLIN **radio contours** are plotted on top and are at 2, 4, 9, 16, 25, 36, 49, 64 mJy/beam. The image correspond to the central $\sim 8 \times 6$ ($\sim 740 \times 550$ pc) of the nucleus of NGC 4151.

Narrow-line emission

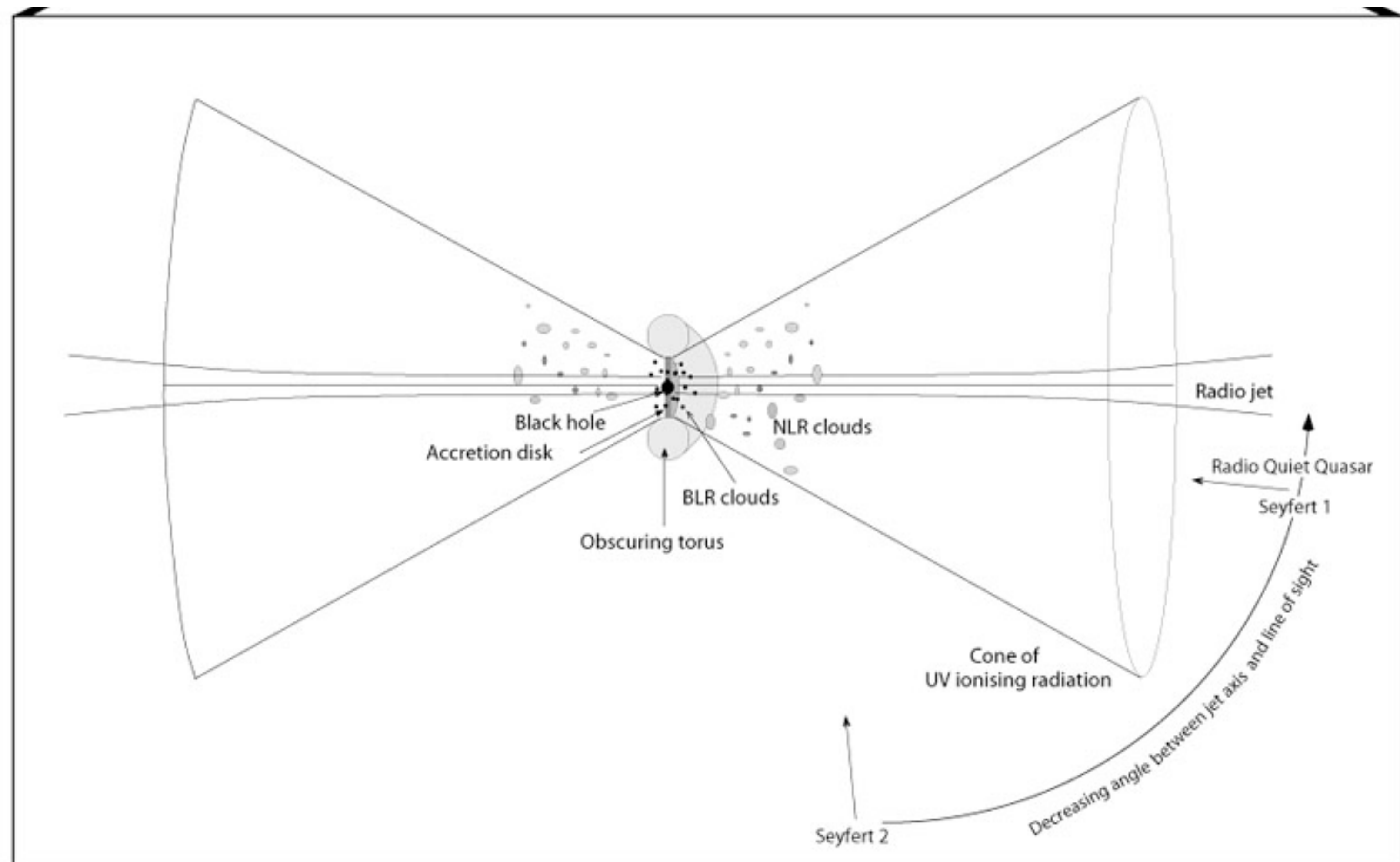
Left: Radio image of neutral hydrogen gas in the spiral Seyfert host galaxy NGC 4151

Right: composite image of the central regions of NGC 4151 showing a 1.4-GHz radio image of the well-collimated plasma jet surrounded by an obscuring torus of molecular hydrogen imaged at 2.2 μ m and an inferred inner ring of neutral hydrogen from absorption measurements.



Narrow-line emission

Sketch of an AGN central engine with a central black hole surrounded by (a) an accretion disc that emits cones of ultraviolet ionising radiation and defines the radio jet launch direction, (b) a torus of dust a gas that accounts for the different observed kinds of radio-quiet AGN by blocking our view of the accretion disc and dense, rapidly-moving ionised gas clouds in the broad-line region (BLR) when viewed edge-on (type 2 objects). Less-dense ionised clouds in the narrow-line region (NLR) lie above the plane of the torus and are visible from all angles.



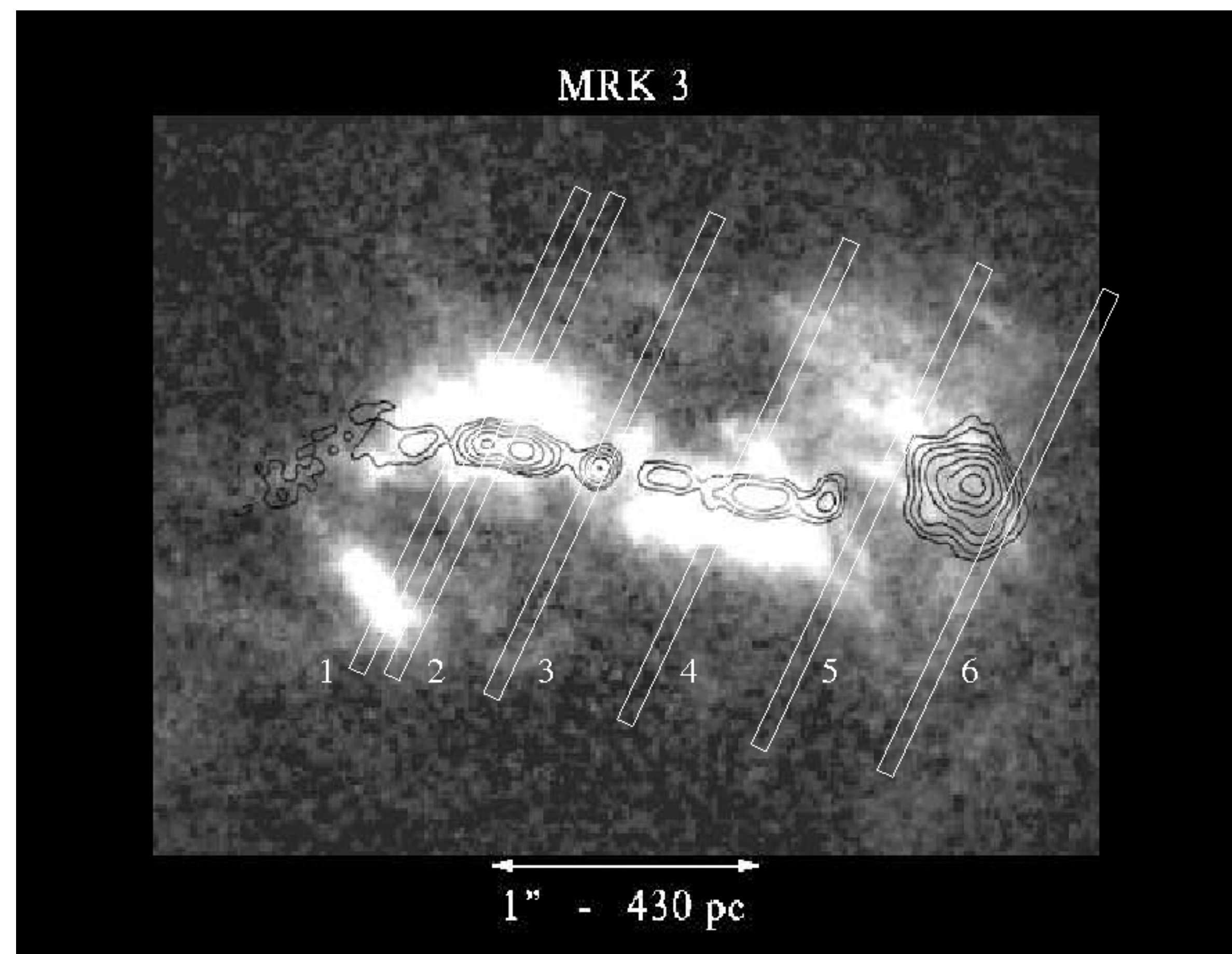
Narrow-line emission

Similar observations have been made of Mrk 3, a Seyfert 2 galaxy. In this case there is additional evidence that the narrow-line region is surrounding the radio jets.

It has been suggested that the material forming the radio jets is expanding at near $0.1c$ from the centre of the galaxy. As the **jets move through the interstellar material, the gas is ionized at a temperature of $\sim 10^7$ K. The overheated gas expands outward away from the jets**, which then produces the narrow-line emission region.

Since the radio jets of Seyfert galaxies are typically only a few kiloparsecs in length, this implies that ages of roughly 10^4 to 10^5 years can be deduced based on the expansion velocity of the jets.

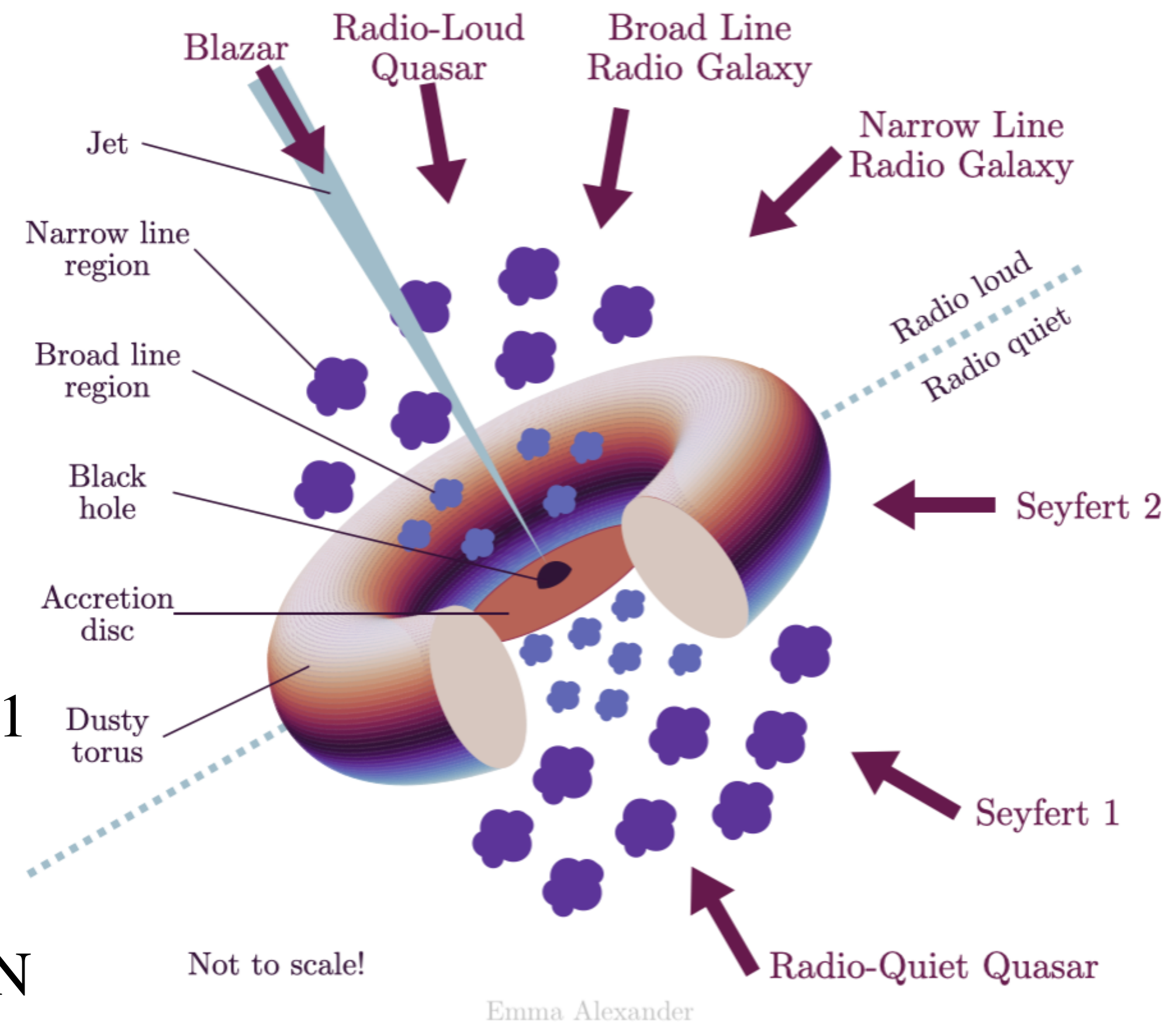
Seyfert phenomena may be relatively transient events, caused by the temporary feeding of the galaxy's supermassive black hole.



HST image of Mrk 3 in the [O III] emission line from Capetti et al. (1996) with superposed the contour radio image from Kukula et al. (1993) and the 6 slit positions where the spectra were taken.

Unified model of AGN

- Its central engine is an accretion disk orbiting a rotating, supermassive black hole.
- The AGN is powered by the conversion of gravitational potential energy into synchrotron radiation, although the rotational kinetic energy of the black hole may also serve as an important energy source.
- The structure of the accretion disk depends on the ratio of the accretion luminosity to the Eddington limit. To supply the observed luminosities, the most energetic AGNs must accrete between about 1 and $10 M_{\odot} \text{ yr}^{-1}$.
- The perspective of the observer, together with the mass accretion rate and mass of the black hole, largely determines whether the AGN is called a Seyfert 1, a Seyfert 2, a BLRG, a NLRG, or a radio-loud or radio-quiet quasar.
- The unified model does appear to provide an important framework for describing many of the general characteristics of active galaxies.



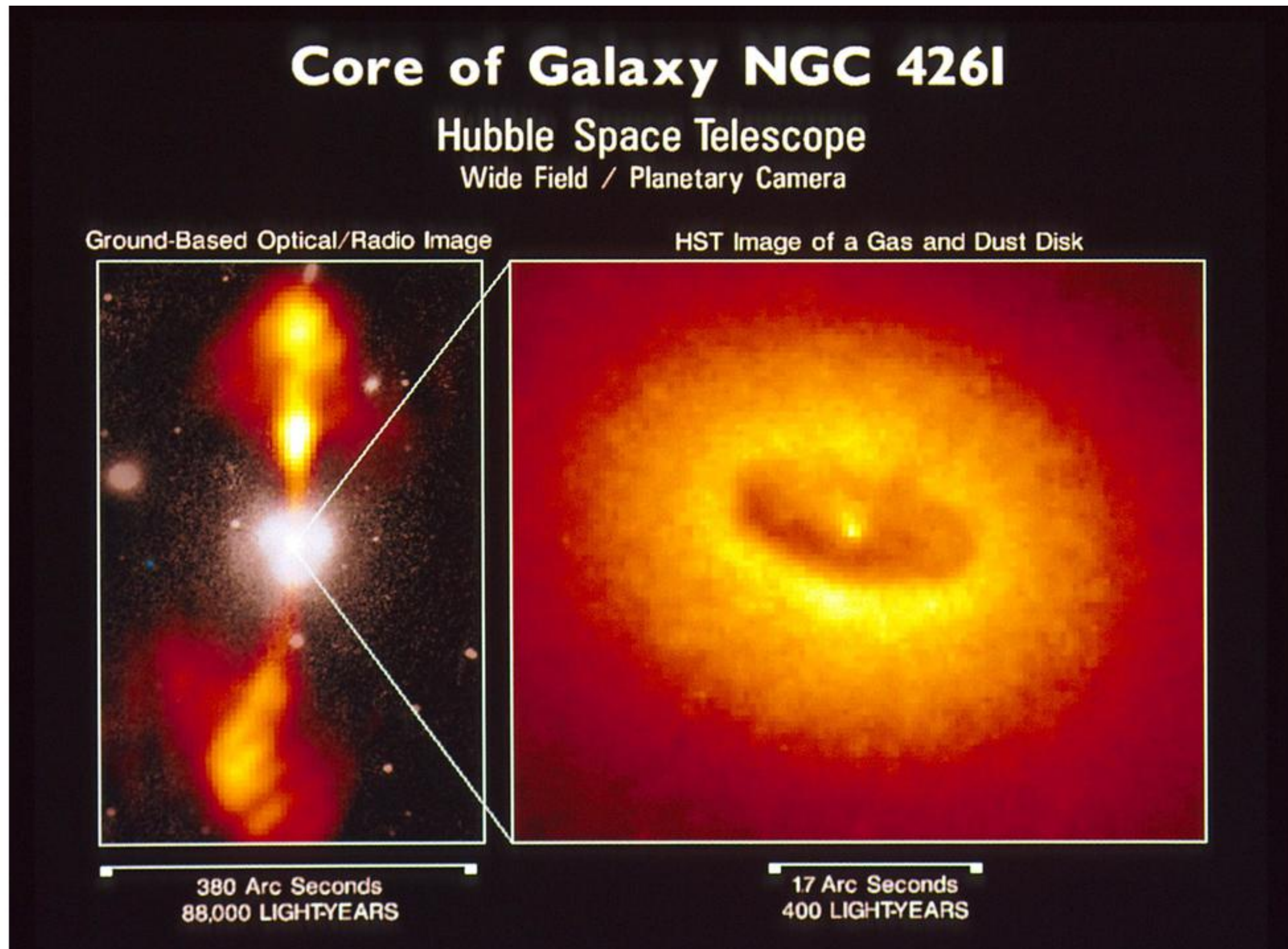
Unified model of AGN

The figure shows an HST image of NGC 4261, an **elliptical radio galaxy** in the Virgo cluster that is classified optically as a **LINER**.

The core of this radio-loud object shows a **bright nucleus** surrounded by a large, **obscuring torus** that is **perpendicular to the radio jets**.

The central object is probably a $10^7 M_\odot$ **black hole**, although the HST image does not have the resolution to confirm this.

The torus has a radius of about 70 pc, and the jets reach out some 15 kpc from the nucleus.



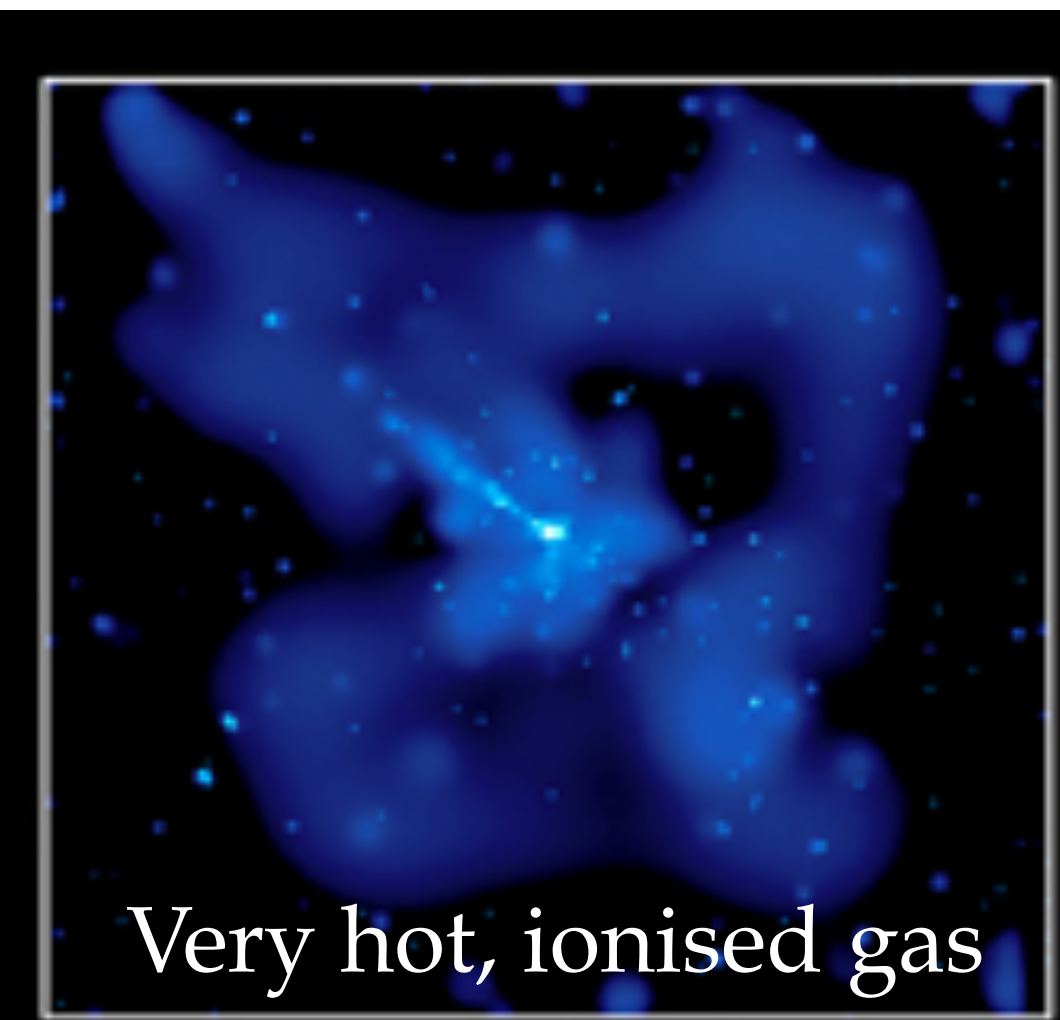
Unified model of AGN

The AGN **Centaurus A**, also known as **NGC 5128**

Observed at different wavelengths.

Dust + HI -> evidence for recent interaction/merger

X-rays + radio -> evidence for AGN activity



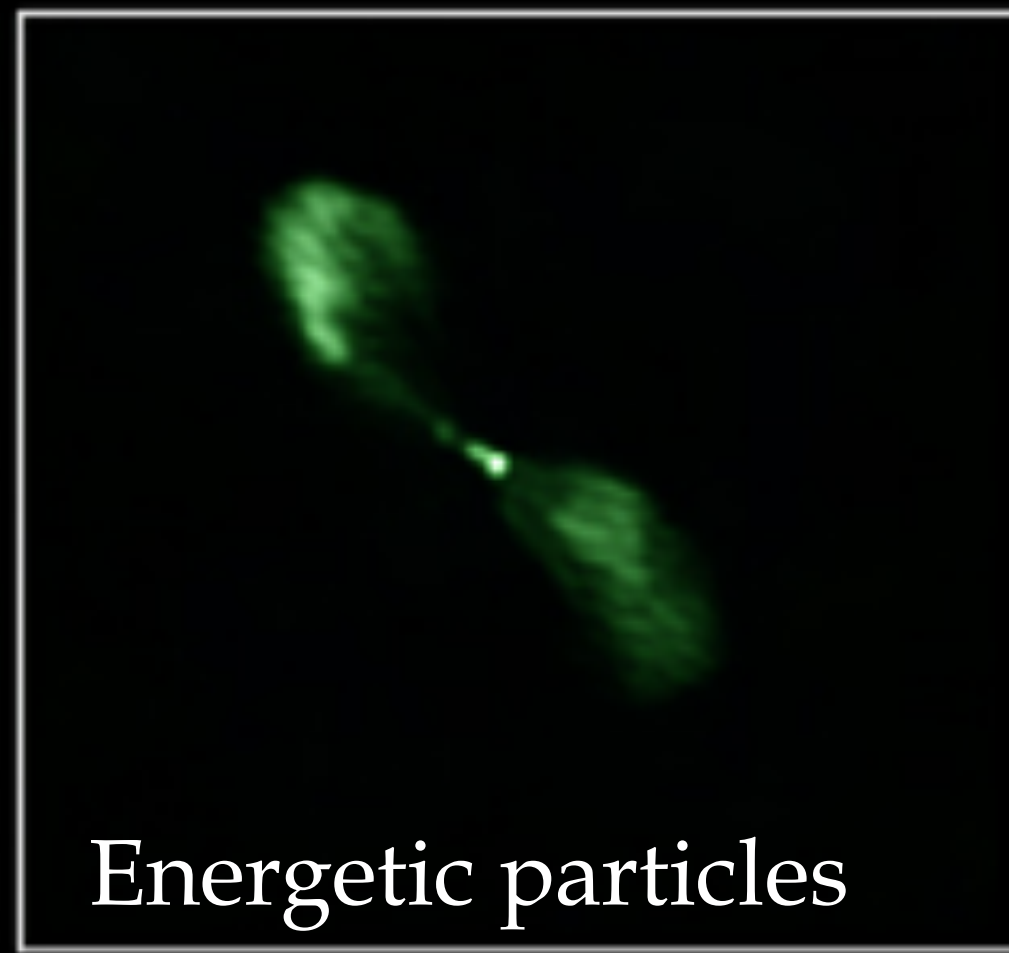
Very hot, ionised gas

CHANDRA X-RAY



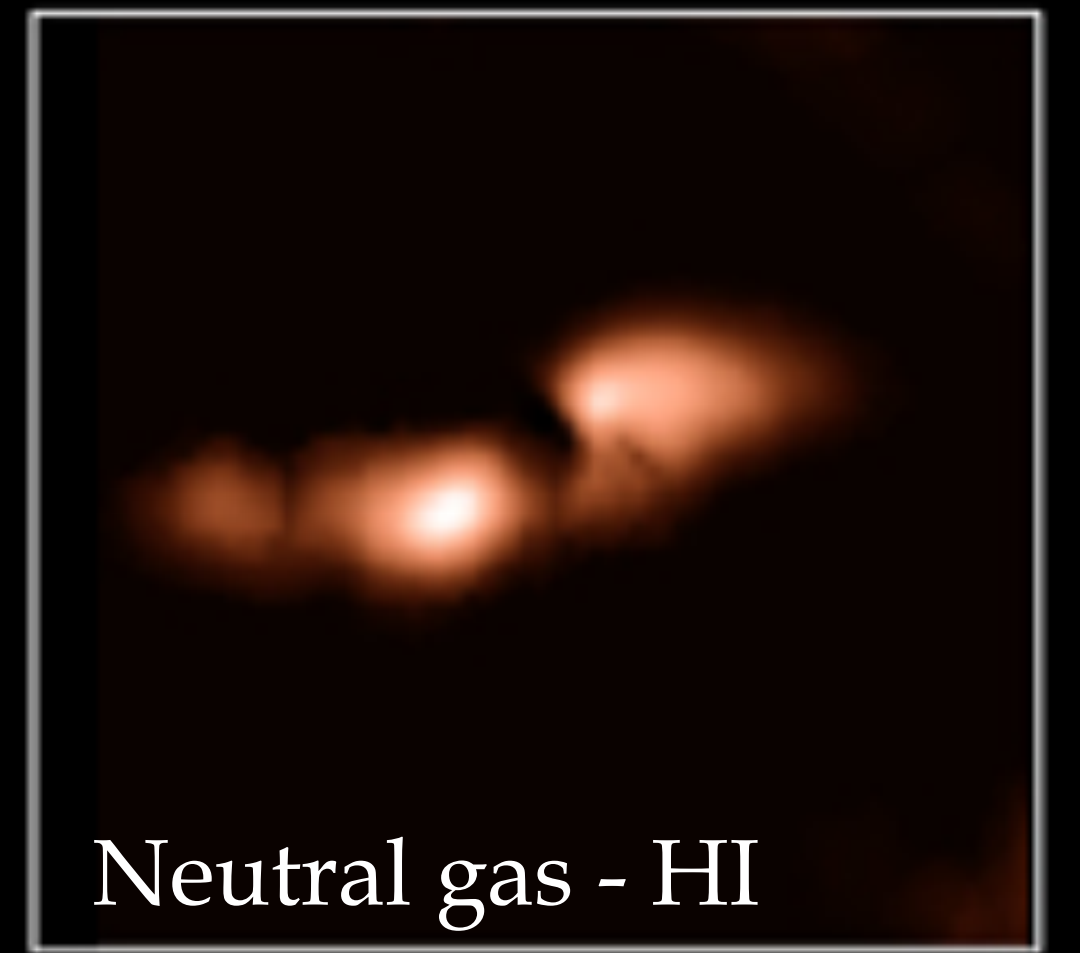
Stars and dust

DSS OPTICAL



Energetic particles

NRAO RADIO
CONTINUUM



Neutral gas - HI

NRAO RADIO
(21-cm)